Renormalization in a classical lattice field theory

Jochen Bartels
*Institute for Nonlinear Science, University of California at San Diego, La Jolla, California 92093 and II. Institut fur Theoretische Physik, Universität Hamburg, West Germany**

Shau-Jin Chang
*Institute for Nonlinear Science, University of California at San Diego, La Jolla, California 92093; La Jolla Institute, La Jolla, California 92037, and Physics Department, University of Illinois at Urbana-Champaign, Urbana, Illinois 61801**

(Received 27 July 1989)

We formulate and describe a renormalization-group transformation for classical $\lambda\phi^4$-field theory on a lattice. The main idea is to divide the angle variables of the oscillators into the fast ones (large momenta) and the slow ones (low momenta) and to average over the fast ones. This results in an effective Hamiltonian for the remaining slow modes, which can be compared with the starting Hamiltonian. We derive fixed-point conditions and obtain a scaling law for those classical solutions for which the renormalization step can be iterated. There is a striking resemblence between our classical treatment and the analogous procedure in quantum field theory, which we discuss in some detail.

I. INTRODUCTION

Renormalization-group transformations provide one of the most powerful tools for studying systems with very large numbers of degrees of freedom such as in statistical mechanics or quantum field theories near phase transition points.[1-3] Following the review article of Kogut and Wilson,[1] a renormalization-group transformation of the parameters of a theory is obtained by integrating out the high-momentum (or small-scale) degrees of freedom. In other words, a change of the ultraviolet cutoff leads to a modification of, say, masses and coupling constants in a quantum field theory. At or near a phase transition point, these changes become particularly simple, and the systems exhibit a scale invariance. Although all these features are not limited by perturbation theory, it is often useful to rephrase them in the language of perturbation theory. Since near a phase transition point the Hamiltonian of the system looks the same after a renormalization-group transformation, it is possible to repeat this transformation many times and one thus effectively carries out the perturbation theory to a very high order.

It is in this spirit that one might ask similar questions about classical systems with large numbers of degrees of freedom. To be definite, we have in mind classical Hamiltonian systems consisting of N weakly coupled harmonic oscillators, such as in a classical field theory on a spatial lattice in a finite volume. In the absence of any interaction such a system is integrable and its trajectory moves on N-tori in $2N$-dimensional pq space. When the interaction is turned on, many of these tori are destroyed but the majority is preserved. The preserved tori are those whose frequencies are sufficiently incommensurable. It has been shown[4,5] that for such frequencies canonical perturbation theory provides meaningful predictions. With increasing strength of the interaction more and more tori are destroyed, and the system eventually becomes chaotic. Now suppose that the parameters of the system are given special values (quite similar to those which make the quantum analog of this system critical), and assume that the coupling is still sufficiently small such that not all Kolmogorov-Arnold-Moser (KAM) tori are destroyed. Then one might ask whether among the preserved tori there are special classical orbits which show some sort of a scaling behavior when looked at at different length scales. Could one use renormalization-group transformations to get information on these trajectories to very-high-order perturbation theory?

The key observation in trying to find an answer to this question is that canonical perturbation theory in classical Hamiltonian mechanics involves time averaging over fast degrees of freedom. It thus very naturally provides a mechanism to do something analogous to the "integration over large momentum degrees of freedom" in Wilson's renormalization-group transformation. For an (oscillating) system which is close to an integrable one

$$H(I,\theta)=H_0(I)+\lambda H_1(I,\theta) \tag{1.1}$$

(I,θ are action and angle variables, H_0 is integrable, and $\lambda \ll 1$), the slow (fast) variables are the I's (the θ's) and obey

$$-\dot{I}_k=\frac{\partial H}{\partial \theta_k}=O(\lambda)\ , \tag{1.2}$$

$$\dot{\theta}_k=\frac{\partial H}{\partial I_k}=\omega_k=O(1) \tag{1.3}$$

($k=1,\ldots,N$). Canonical perturbation theory is based upon averaging over the θ's. If, moreover, there is a strong ordering in the frequences

$$\omega_1 \ll \omega_2 \ll \cdots \ll \omega_N\ , \tag{1.4}$$

then we have an additional division of the angles into fast and slow ones. It is then very suggestive to first average over a certain group of the fastest θ's (large ω), then to move on to a second group of slower θ's, and so on. After each step, one ends up with a reduced Hamiltonian which describes the effective interaction of the remaining slower modes in the presence of the (averaged) fast modes. Following the spirit of Wilson's renormalization-group analysis in the vicinity of a critical point, one then might search for a situation where this reduced Hamiltonian is of the same form as the one before the averaging. One would expect that this leads to restrictions on the parameters of the systems, but one may also single out a special subset of classical solutions (i.e., with special initial conditions). In analogy to what has been said above about the quantum-field-theory case, such a procedure would allow one, at least for this selected set of classical solutions, to carry out perturbation theory to very high orders. We would, therefore, be in a much better situation than by applying canonical perturbation theory in (1.1) to all angle variables at the same time, because such an approach would have to stop at some finite order in λ.

In this paper we attempt to apply this idea to a system of weakly coupled harmonic oscillators, namely, a classical $\lambda\phi^4$ field theory on a lattice (with a finite spatial volume). This model is sufficiently simple for us to carry out low-order calculations easily, and it has widely been studied in quantum field theory and statistical mechanics. In order to obtain a nontrivial fixed point for the coupling constant, one has to work in $D=3-\epsilon$ spatial dimensions. This has to be done in the limit of very large lattice volumes where sums over discrete momenta can be approximated by momentum integrals. More interesting models are lattice gauge theories, but the complications connected with the gauge invariance suggest that it might be a better idea to start with a less sophistical toy model.

The main purpose of this paper is a detailed description of renormalization-group transformations in this classical Hamiltonian system. As it was said before, its main part consists of averaging over a set of fast angles (which belong to the large-momentum degrees of freedom). This results in an effective Hamiltonian for the remaining slower variables (belonging to small momenta). In order to be able to compare this new Hamiltonian with the starting one, two further canonical transformations and a rescaling of momenta are necessary. It turns out that details of all these steps are very similar to the analogous renormalization-group transformation in $\lambda\phi^4$ field theory: this includes the appearance of diagrams with closed momentum loops (Feynman diagrams) and the concept of mass and wave-function renormalization. The question about under what conditions the resulting Hamiltonian has the same form as the starting Hamiltonian leads to fixed-point conditions on the coupling constant and on the mass. The detailed form of these equations is again very similar to those obtained in the quantum field theory. The further requirement that this renormalization step can be iterated without leaving the fixed point leads to a restriction on those classical solutions for which this procedure works: we obtain a scaling law for the field amplitudes which is reminiscent of the scaling laws for the Green's functions in quantum field theory (or the correlation functions in statistical mechanics) near a critical point.

We interpret this result as follows. Among the KAM tori which are preserved in the presence of the interaction terms λH_1 there seems to exist a special set of regular classical solutions which, at or near the fixed point, behave the same way as the quantum system does near the critical point. In this sense the classical system (i.e., some of its solutions) seems to "know" about the critical behavior of the quantum system. We cannot say at the moment how important these solutions are for the computation of a partition function, but questions along this line certainly deserve further attention.

It should be stated rather clearly that our analysis does not attempt to provide any rigorous proof for the existence of these special classical solutions. In this paper we rather intended to formulate the ideal and to work out in some detail how renormalization might work in a classical lattice field theory. A more rigorous analysis would certainly be difficult. Apart from the fact that the existing proofs of KAM theory[4,5] for systems with $N>2$ degrees of freedom do not allow us to take the limit $N\to\infty$, our model also has the slight complication that the frequencies of the free Hamiltonian are constants, i.e., they do not depend upon the action variables. Since such a dependence will come in as a result of the interaction term, one should redefine the free part of the Hamiltonian by absorbing parts of the interaction into it. In order to keep our calculations as easy as possible, we have chosen to ignore this complication for the moment. But we feel that at some later stage our analysis should be refined to take care of this feature.

This paper will be organized as follows. We begin (Sec. II) with a simple example which illustrates how averaging over a fast mode leads to a renormalization for the parameters of the slow mode. Section III contains the main part of this paper: it describes one complete renormalization group transformation for the $\lambda\phi^4$ model. In Sec. IV we derive scaling laws for those trajectories for which a fixed-point situation can be reached. Section V contains a discussion of our results. Some details of our calculations are put into two appendixes.

II. COUPLED OSCILLATORS

We consider a pair of coupled harmonic oscillators described by the Hamiltonian,

$$H=\tfrac{1}{2}p_1^2+\tfrac{1}{2}\omega_1^2q_1^2+\tfrac{1}{2}p_2^2+\tfrac{1}{2}\omega_2^2q_2^2+\frac{\lambda}{4}(q_1^2+q_2^2)^2\ . \tag{2.1}$$

The equations of motion for q_1 and q_2 are

$$\ddot{q}_1+\omega_1^2q_1+\lambda(q_1^2+q_2^2)q_1=0\ , \tag{2.2}$$

$$\ddot{q}_2+\omega_2^2q_2+\lambda(q_1^2+q_2^2)q_2=0\ . \tag{2.3}$$

We assume that $\omega_1^2\ll\omega_2^2$, and that the energy of the system is small such that $\lambda(q_1^2+q_2^2)\approx\omega_1^2\ll\omega_2^2$. Under these assumptions, the motion of q_1 is much slower than that of q_2. We shall refer to q_1 as the slow mode and q_2 as the

fast mode. The relative time scales are characterized by a small parameter

$$\epsilon \equiv \omega_1/\omega_2 \ll 1 \ . \tag{2.4}$$

We first consider the fast motion and write (2.3) as

$$\ddot{q}_2 + \Omega^2 q_2 + \lambda q_2^3 = 0 \ , \tag{2.5}$$

with

$$\Omega^2 \equiv \omega_2^2 + \lambda q_1(t)^2 \ . \tag{2.6}$$

Comparing with the fast motion of q_2, we can view Ω as a function of a slow time scale, $\tilde{t} \equiv \epsilon t$. To the lowest approximation, we can treat $\Omega(\tilde{t})$ as a constant. Then, the solution to (2.5) with an appropriate initial phase is an elliptical function[6]

$$q_2 = A(\tilde{t})\mathrm{cn}(\dot{B}(\tilde{t}), \nu(\tilde{t})) \ , \tag{2.7}$$

where A, ν, and $\dot{B}$ are functions of $\tilde{t}$.

Comparing (2.5) with the identity

$$\frac{d^2\mathrm{cn}(x,\nu)}{dx^2} + (1-2\nu)\mathrm{cn}(x,\nu) + 2\nu\,\mathrm{cn}^3(x,\nu) = 0 \ , \tag{2.8}$$

we obtain the relations

$$\Omega^2(\tilde{t}) = [1-2\nu(\tilde{t})]\dot{B}(\tilde{t})^2 \ , \tag{2.9}$$

$$\lambda A(\tilde{t})^2 = 2\nu(\tilde{t})\dot{B}(\tilde{t})^2 \ . \tag{2.10}$$

We can solve for ν and $\dot{B}$ in terms of $\Omega(\tilde{t})$ and $A(\tilde{t})$ as

$$\nu(\tilde{t}) = \frac{\lambda A(\tilde{t})^2}{2\Omega(\tilde{t})^2 + 2\lambda A(\tilde{t})^2} \ , \tag{2.11}$$

$$\dot{B}(\tilde{t})^2 = \Omega(\tilde{t})^2 + \lambda A(\tilde{t})^2 \ . \tag{2.12}$$

To determine the slow time dependence of $A(\tilde{t})$, we evaluate the action

$$I_2(\tilde{t}) \equiv \frac{1}{2\pi}\oint p_2 dq_2 = \tfrac{1}{2}A(\tilde{t})^2\dot{B}(\tilde{t})C(\nu(\tilde{t})) \ , \tag{2.13}$$

with

$$C(\nu) \equiv \frac{4}{\pi}\int_0^{K(\nu)} du\ \mathrm{sn}^2(u,\nu)\mathrm{dn}^2(u,\nu) = \frac{4}{3\pi\nu}[(1-\nu)K(\nu) - (1-2\nu)E(\nu)] = 1 - \tfrac{3}{8}\nu - \tfrac{5}{64}\nu^2 + \cdots \ , \tag{2.14}$$

where $K(\nu)$ and $E(\nu)$ are the complete elliptical integrals of the first and the second kind. Using (2.11)–(2.13), we can determine A, ν, and $\dot{B}$ as functions of Ω and I_2. The adiabatic invariance theorem[5,7] tells us that δI_2, the change of I_2 per slow cycle, vanishes to order ϵ. Actually for an analytic $\Omega(\tilde{t})$, δI_2 vanishes exponentially as $\exp(-\mathrm{const}/\epsilon)$. In particular, the faster the variable q_2 is, the better the adiabatic invariance I_2 becomes. Thus we can treat $I_2(\tilde{t})$ as a constant even for the slow motion of q_1.

For the motion of q_1 in (2.2), we can separate the q_2^2 term into an averaged value $\langle q_2^2 \rangle$ and a fluctuation term. The fluctuation term gives only a small effect on the motion of q_1, and may be ignored.[8] We obtain an approximate equation for q_1,

$$\ddot{q}_1 + (\omega_1^2 + \lambda\langle q_2^2\rangle)q_1 + \lambda q_1^3 = 0 \ . \tag{2.15}$$

The expectation value of q_2^2 is

$$\langle q_2^2 \rangle = A^2\langle \mathrm{cn}^2(B,\nu)\rangle = \tfrac{1}{2}A(\tilde{t})^2 D(\nu) \ , \tag{2.16}$$

with

$$D(\nu) \equiv \frac{2}{K(\nu)}\int_0^{K(\nu)} du\ \mathrm{cn}^2(u,\nu) = \frac{2}{\nu K(\nu)}[E(\nu) - (1-\nu)K(\nu)] = 1 - \tfrac{1}{8}\nu - \tfrac{1}{16}\nu^2 + \cdots \ . \tag{2.17}$$

Since $A(t)$ and $\nu(t)$ depend on $q_1(t)$ through $\Omega(t)$, $\lambda\langle q_2^2\rangle q_1$ represents an additional interaction due to the fast mode q_2. The above result is valid for all λ and depends only on the smallness of ϵ. In the following, we find it instructive to treat the reduction problem as a perturbation in λ. For small λ, (2.11)–(2.16) give

$$\nu = \frac{\lambda I_2}{\omega_2^3} + O(\lambda^2) \ , \tag{2.18}$$

$$A^2 = \frac{2I_2}{\omega_2}\left[1 - \frac{5\lambda I_2}{8\omega_2^3} - \frac{\lambda q_1^2}{2\omega_2^2} + O(\lambda^2)\right] \ , \tag{2.19}$$

$$\dot{B}^2 = \omega_2^2 + \frac{2\lambda I_2}{\omega_2} + \lambda q_1^2 + O(\lambda^2) \ , \tag{2.20}$$

$$\langle q_2^2 \rangle = \frac{I_2}{\omega_2}\left[1 - \frac{3\lambda I_2}{4\omega_2^3} - \frac{\lambda q_1^2}{2\omega_2^2} + O(\lambda^2)\right] \ . \tag{2.21}$$

The q_1 equation becomes

$$\ddot{q}_1 + \left[\omega_1^2 + \frac{\lambda I_2}{\omega_2}\right]q_1 + \left[\lambda - \frac{\lambda^2 I_2}{2\omega_2^3}\right]q_1^3 = 0 \ . \tag{2.22}$$

Equation (2.22) indicates that the most important effect of the fast mode on q_1 is to change the effective frequency ω_1^2 and the coupling constant λ. These are the analogs of the mass and the coupling constant renormalization.

Physically, we can also understand the separation of coupled fast and slow oscillators into two independent motions as follows. For small λ and ϵ, the system is nearly integrable. We can treat the fast mode as a clock, and describe the motion of the slow mode by a sequence of points at $\theta_2 = 0$, $\mathrm{mod}2\pi$, as in a Poincaré return map.[9] Then, the motion of q_1 is one dimensional if its trajectory lies on a KAM curve, and is approximately one dimensional if its motion is trapped between two adjacent KAM curves. Since most of the trajectories are on or near a KAM curve for small ϵ and λ, we expect our approximation to be good.

In the following, we shall treat our system by the canonical perturbation theory.[9] We write H as

$$H = H_0 + \lambda H_1 \ , \tag{2.23}$$

with

$$H_0=\tfrac{1}{2}p_1^2+\tfrac{1}{2}\omega_1^2q_1^2+\tfrac{1}{2}p_2^2+\tfrac{1}{2}\omega_2^2q_2^2\ , \tag{2.24}$$

$$H_1=\tfrac{1}{4}(q_1^2+q_2^2)^2\ . \tag{2.25}$$

Introducing the action and angle variables I_i and θ_i for H_0,

$$q_i=\sqrt{2I_i/\omega_i}\cos\theta_i\ , \tag{2.26}$$

$$p_i=-\sqrt{2\omega_iI_i}\sin\theta_i\ , \tag{2.27}$$

we have

$$H_0(I)=I_1\omega_1+I_2\omega_2\ , \tag{2.28}$$

$$H_1(I,\omega)=\left[\frac{I_1}{\omega_1}\cos^2\theta_1+\frac{I_2}{\omega_2}\cos^2\theta_2\right]^2\ . \tag{2.29}$$

We assume as before that $\omega_1^2\ll\omega_2^2$. We shall make a canonical transformation to remove the fast variable θ_2 in H. We introduce a generating function

$$F_2(I',\theta)=I_1'\theta_1+I_2'\theta_2+\lambda S_1(I',\theta)+\lambda^2S_2(I',\theta)+\cdots\ . \tag{2.30}$$

The generating function F_2 leads to the canonical transformation

$$I_i=I_i'+\lambda\frac{\partial S_1(I',\theta)}{\partial\theta_i}+\lambda^2\frac{\partial S_2(I',\theta)}{\partial\theta_i}+\cdots\ , \tag{2.31}$$

$$\theta_i'=\theta_i+\lambda\frac{\partial S_i(I',\theta)}{\partial I_i'}+\lambda^2\frac{\partial S_2(I',\theta)}{\partial I_i'}+\cdots\ . \tag{2.32}$$

In terms of the new variables I' and θ', we have

$$H=H_0(I')+\lambda\left[\omega_i\frac{\partial S_1(I',\theta')}{\partial\theta_i'}+H_1(I',\theta')\right]+\lambda^2\left[\omega_i\frac{\partial}{\partial\theta_i'}\left[S_2-\frac{1}{2}\frac{\partial S_1}{\partial I'}\frac{\partial S_1}{\partial\theta'}\right]+H_2\right]+\cdots\ , \tag{2.33}$$

with

$$H_2\equiv\left\{S_1,H_1+\frac{1}{2}\omega_i\frac{\partial S_1}{\partial\theta_i'}\right\}\ , \tag{2.34}$$

and the curly brackets represent the Poisson brackets.

We now separate H_1 into an expectation value with respect to θ_2' and an oscillating part $\tilde{H}_1$,

$$H_1=\langle H_1\rangle+\tilde{H}_1(I',\theta')\ , \tag{2.35}$$

with

$$\begin{aligned}\langle H_1\rangle&=\frac{I_1'^2}{\omega_1^2}\cos^4\theta_1'+\frac{2I_1'I_2'}{\omega_1\omega_2}\cos^2\theta_1'\langle\cos^2\theta_2'\rangle+\frac{I_2'^2}{\omega_2^2}\langle\cos^4\theta_2'\rangle\\&=\frac{I_1'^2}{\omega_1^2}\cos^4\theta_1'+\frac{I_1'I_2'}{\omega_1\omega_2}\cos^2\theta_1'+\frac{3I_2'^2}{8\omega_2^2}\ .\end{aligned} \tag{2.36}$$

We choose an S_1 to cancel the oscillatory part $\tilde{H}_1$. Given S_1, we can compute H_2. We choose an S_2 to cancel the oscillatory part of H_2, etc. In the following, we shall suppress the primes on these variables, and just remember that all variables are primed variables. We can obtain S_1 and $\langle H_2\rangle$ straightforwardly as

$$S_1=-\frac{I_1I_2\sin(2\theta_1)(\cos(2\theta_2)}{4\omega_2(\omega_1^2-\omega_2^2)}+\left[\frac{I_1I_2\cos(2\theta_1)}{4\omega_1(\omega_1^2-\omega_2^2)}-\frac{I_1I_2}{4\omega_1\omega_2^2}-\frac{I_2^2}{4\omega_2^3}\right]\sin(2\theta_2)-\frac{I_2^2}{32\omega_2^3}\sin(4\theta_2)\ , \tag{2.37}$$

$$\begin{aligned}\langle H_2\rangle\equiv&-\frac{17I_2^3}{64\omega_2^5}+\frac{I_1^2I_2}{8\omega_1^2\omega_2}\left[\frac{\cos(2\theta_1)}{\omega_1^2-\omega_2^2}-\frac{1}{\omega_2^2}\right][1+\cos(2\theta_1)]\\&+\frac{I_1I_2^2}{16\omega_1\omega_2^2}\left[-\frac{1+\cos(2\theta_1)}{\omega_1^2-\omega_2^2}+3\left[\frac{\cos(2\theta_1)}{\omega_1^2-\omega_2^2}-\frac{1}{\omega_2^2}\right]-\frac{3}{\omega_2^2}[1+\cos(2\theta_1)]\right]\ .\end{aligned} \tag{2.38}$$

To $O(\lambda^2)$ and in terms of I_2, p_1 and q_1, the new Hamiltonian is

$$\begin{aligned}H'&=H_0(I)+\lambda\langle H_1\rangle+\lambda^2\langle H_2\rangle\\&=I_2\omega_2+\tfrac{1}{2}p_1^2+\tfrac{1}{2}\omega_1^2q_1^2+\lambda\left[\frac{3I_2^2}{8\omega_2^2}+\frac{I_2}{2\omega_2}q_1^2+\frac{1}{4}q_1^4\right]\\&\quad+\lambda^2\left[-\frac{17I_2^3}{64\omega_2^5}-\frac{I_2^2q_1^2}{32\omega_2^2}\left[-\frac{1}{\omega_1^2-\omega_2^2}+\frac{9}{\omega_2^2}\right]-\frac{3I_2^2p_1^2}{32\omega_1^2\omega_2^2}\left[\frac{1}{\omega_1^2-\omega_2^2}+\frac{1}{\omega_2^2}\right]+\frac{I_2q_1^4}{16\omega_2}\left[\frac{1}{\omega_1^2-\omega_2^2}-\frac{1}{\omega_2^2}\right]\right.\\&\quad\left.-\frac{I_2q_1^2p_1^2}{16\omega_1^2\omega_2}\left[\frac{1}{\omega_1^2-\omega_2^2}+\frac{1}{\omega_2^2}\right]\right]+O(\lambda^3)\ .\end{aligned} \tag{2.39}$$

The absence of θ_2 in H' indicates that to this order I_2 is a constant. It is pleasing to see that the $\langle H_1 \rangle$ term gives rise to the mass (frequency) renormalization as shown in (2.22). The first terms in $\langle H_1 \rangle$ and $\langle H_2 \rangle$ contribute to the adiabatic invariance associated with θ_2. They change the frequency ω_2 but do not affect the equation of motion of q_1. The second term of $\langle H_2 \rangle$ gives a second-order mass renormalization, and the third term gives a wave-function renormalization. The fourth term leads to a coupling constant renormalization, which, in the limit $\omega_1^2 \ll \omega_2^2$, reproduces the correction in (2.22). The last term represents a new kind of vertex which is intrinsic to the use of the Hamiltonian formulation and the old fashioned perturbation theory. All the terms mentioned above will appear in the reduction of classical field theories which will be the topic of Sec. III.

III. A RENORMALIZATION-GROUP TRANSFORMATION

We now turn to classical $\lambda\phi^4$ theory. By putting the theory on a spatial periodic lattice with lattice spacing a, and by keeping the volume finite [length of the cubic lattice is $L=a(2N+1)$], we have both an ultraviolet and an infrared cutoff. The Hamiltonian is

$$H=\sum_l \left[\frac{1}{2}\pi_l^2+\frac{1}{2}m^2\phi_l^2+\frac{1}{2}\sum_{i=1}^{3}(\phi_{l+i}-\phi_l)^2+\frac{\lambda}{4!}\phi_l^4\right] . \tag{3.1}$$

The summation extends over all lattice points l and for convenience we have put $a=1$. A Fourier transformation

$$\phi_l=\frac{1}{L^D}\sum_{\mathbf{k}} e^{i\mathbf{k}\cdot l}\phi_{\mathbf{k}} , \tag{3.2}$$

with

$$\mathbf{k}=\frac{2\pi}{L}\mathbf{n}, \quad \mathbf{n}=(n_1,n_2,n_3), \quad |n_i|\le N \tag{3.3}$$

diagonalizes the free part of the Hamiltonian:

$$H=\frac{1}{L^D}\sum_{\mathbf{k}}\tfrac{1}{2}[\pi_{\mathbf{k}}\pi_{-\mathbf{k}}+\omega^2(\mathbf{k})\phi_{\mathbf{k}}\phi_{-\mathbf{k}}] + \frac{1}{L^{3D}}\frac{\lambda}{4!}\sum_{\{\mathbf{k}\}}\phi_{\mathbf{k}_1}\cdots\phi_{\mathbf{k}_4} . \tag{3.4}$$

Here $D=3$ and

$$\omega^2(\mathbf{k})=m^2+4\sum_{i=1}^{3}\sin^2\frac{k_i}{2} . \tag{3.5}$$

The complex-valued variables $\phi_{\mathbf{k}}$ and $\pi_{\mathbf{k}}$ satisfy $\pi_{-\mathbf{k}}=\pi_{\mathbf{k}}^*$, $\phi_{-\mathbf{k}}=\phi_{\mathbf{k}}^*$. In the interaction part of (3.4), the summation symbol includes a momentum-conserving δ function

$$\sum_{\mathbf{n}}\delta^3(\mathbf{k}_1+\mathbf{k}_2+\mathbf{k}_3+\mathbf{k}_4+2\pi\mathbf{n}) .$$

In principle, we could write our Hamiltonian in terms of real and imaginary parts of ϕ and π, and all calculations would give real-valued results. However, it turns out to be much more convenient to switch to other, complex-valued variables $a(\mathbf{k})$ and $a^*(\mathbf{k})$, which are the classical analogs of annihilation and creation operators in quantum field theory.[10] For each $\mathbf{k}$ one defines

$$a(\mathbf{k})=\frac{L^{-D/2}}{\sqrt{2}}\left[\sqrt{\omega(\mathbf{k})}\phi_{\mathbf{k}}+\frac{i}{\sqrt{\omega(\mathbf{k})}}\pi_{\mathbf{k}}\right] \tag{3.6}$$

and, correspondingly, its complex conjugate $a^*(\mathbf{k})$. The canonical transformation which takes us from $\phi_{\mathbf{k}},\pi_{\mathbf{k}}$ to $a(\mathbf{k}),a^*(\mathbf{k})$ [$a(\mathbf{k})$ plays the role of new coordinates, $ia^*(\mathbf{k})$ are the new momenta] has the generating function

$$F_2(a^*,\phi)=\sum_{\mathbf{k}\in\Sigma}\left[-\frac{i}{2}L^{-D}\omega(\mathbf{k})\phi_{\mathbf{k}}\phi_{-\mathbf{k}} + i\sqrt{2\omega(\mathbf{k})}L^{-D/2}a^*(\mathbf{k})\phi_{\mathbf{k}} - \tfrac{1}{2}a^*(\mathbf{k})a^*(-\mathbf{k})\right] . \tag{3.7}$$

The new variables have canonical Poisson brackets

$$\{a(\mathbf{k}),a^*(\mathbf{k}')\}=-i\delta_{\mathbf{k}\mathbf{k}'} , \tag{3.8}$$

and the free part of the Hamiltonian takes the form

$$H_0=\sum_{\mathbf{k}}\omega(\mathbf{k})a(\mathbf{k})a^*(\mathbf{k}) . \tag{3.9}$$

For these new variables we now introduce action and angle variables $I(\mathbf{k}),\theta(\mathbf{k})$ (both real-valued)

$$a(\mathbf{k})=\sqrt{I(\mathbf{k})}\,e^{-i\theta(\mathbf{k})} , \tag{3.10}$$

such that

$$H_0=\sum_{\mathbf{k}}\omega(\mathbf{k})I(\mathbf{k}) . \tag{3.11}$$

Connection with the variables $\phi_{\mathbf{k}},\pi_{\mathbf{k}}$ is made through

$$\phi_{\mathbf{k}}=\frac{L^{D/2}}{\sqrt{2\omega(\mathbf{k})}}[\sqrt{I(\mathbf{k})}\,e^{-i\theta(\mathbf{k})}+\sqrt{I(-\mathbf{k})}\,e^{i\theta(-\mathbf{k})}]$$
$$\pi_{\mathbf{k}}=(-i)L^{D/2}\sqrt{\omega(\mathbf{k})/2}[\sqrt{I(\mathbf{k})}e^{-i\theta(\mathbf{k})} - \sqrt{I(-\mathbf{k})}e^{i\theta(-\mathbf{k})}] . \tag{3.12}$$

The Hamiltonian becomes

$$H=\sum_{\mathbf{k}}\omega(\mathbf{k})I(\mathbf{k}) + \frac{\lambda}{4!}\frac{1}{L^D}\sum_{\{\mathbf{k}\}}\prod_{i=1}^{4}\left[\frac{1}{\sqrt{2\omega(\mathbf{k}_i)}}[\sqrt{I(\mathbf{k}_i)}e^{-i\theta(\mathbf{k}_i)} + \sqrt{I(-\mathbf{k}_i)}e^{i\theta(-\mathbf{k}_i)}]\right] . \tag{3.13}$$

This defines our starting Hamiltonian. It will sometimes be convenient to write H in terms of variables a,a^*:

$$H=\sum_{\mathbf{k}}\omega(\mathbf{k})a(\mathbf{k})a^*(\mathbf{k}) + \frac{\lambda}{4!L^D}\sum_{\{\mathbf{k}\}}\prod_{i=1}^{4}\frac{1}{\sqrt{2\omega(\mathbf{k}_i)}}[a(\mathbf{k}_i)+a^*(-\mathbf{k}_i)] . \tag{3.14}$$

In the main part of our paper, we shall use action and angle variables I,θ. Calculations which are described in Appendix B are carried out in terms of the a and a^*'s.

In the following we will apply the idea of Sec. II to the Hamiltonian (3.4): we will average over the "fast" modes (large momenta), and this will lead to an effective Hamiltonian for the "slow" modes (low momenta) with renormalized parameters λ and m. Our aim will then be to bring this Hamiltonian into a form which allows a comparison with out starting Hamiltonian (3.4). This can be done through a few canonical transformations which turn out to be the classical analog of "wave-function renormalization" and "mass renormalization" in quantum field thoery. Together with the averaging procedure, these canonical transformations define what we will name a "renormalization-group transformation." In Sec. IV we then will study under what conditions the new Hamiltonian is the same as the old one: this requires that mass m and coupling λ take certain fixed-point values which depend upon the adiabatic invariants of the fast modes. In order to obtain a nontrivial fixed point for our $\lambda\phi^4$ model, we have to invoke Wilson's idea of working in $D=3-\epsilon$ (spatial) dimensions: for sufficiently large volume ($L\gg 1$) all sums over momenta can be approximated by integrals which allow a continuation in D away from $D=3$. Finally, the requirement that after several renormalization transformations we are still on the fixed point imposes certain restrictions on the classical trajectories: the type of scale invariance that we are looking for only works for special classical orbits.

"Fast" and "slow" modes ("large" and "small" momenta) are defined as follows. Let Λ denote the full range of momenta:

$$\Lambda=\left\{\mathbf{k}\,|\,0\le|k_x|,|k_y|,|k_z|\le\frac{\pi}{a}\right\}. \tag{3.15}$$

The "slow" modes are defined to belong to "low" momenta $\mathbf{k}\in\Lambda_<$, where

$$\Lambda_<=\left\{\mathbf{k}\,|\,0\le|k_x|,|k_y|,|k_z|\le p\frac{\pi}{a}\right\}. \tag{3.16}$$

Correspondingly, "fast" modes belong to "large" momenta $\mathbf{k}\in\Lambda_>$ with

$$\Lambda_>=\Lambda-\Lambda_< . \tag{3.17}$$

To be definite, we take $p=\frac{1}{2}$. In order to make the following presentation as transparent as possible we proceed in two steps: first we give a general description of the transformations which go into a renormalization-group transformation, and in the second part we present the necessary calculations.

A. General description of a renormalization-group transformation

The renormalization-group transformation, which we will describe in the following, consists of four steps: (i) the averaging over the fast modes (large momenta); (ii) mass renormalization; (iii) wave-function renormalization; and (iv) rescaling of momenta. The first three steps are canonical transformations, whereas the fourth one involves rescaling of all dimensional quantities.

We begin with the first step, the integration over the large-$\mathbf{k}$ modes. Write (3.13) as

$$H=H_0(I)+\lambda H_1(I,\theta) \tag{3.18}$$

and decompose H_1 into an averaged part and the remainder (oscillatory part)

$$H_1(I,\theta)=\langle H_1(I,\theta)\rangle+\tilde{H}_1(I,\theta) . \tag{3.19}$$

In the first term, the averaging prescription only refers to those $\theta(\mathbf{k})$ for which $\mathbf{k}\in\Lambda_>$; as a result of this, $\langle H_1\rangle$ will still depend upon the $\theta(\mathbf{k})$ with $\mathbf{k}\in\Lambda_<$. For simplicity, we use the subscripts $<$ and $>$ to distinguish between the two sets of degrees of freedom. We seek a canonical transformation of the form

$$S(I',\theta)=\sum_{\mathbf{k}} I'(\mathbf{k})\theta(\mathbf{k})+\lambda S_1(I',\theta)+\lambda^2 S_2(I',\theta) , \tag{3.20}$$

with

$$I(\mathbf{k})=I'(\mathbf{k})+\lambda\frac{\partial S_1}{\partial\theta(\mathbf{k})}+\lambda^2\frac{\partial S_2}{\partial\theta(\mathbf{k})} \tag{3.21}$$

and

$$\theta'(\mathbf{k})=\theta(\mathbf{k})+\lambda\frac{\partial S_1}{\partial I'(\mathbf{k})}+\lambda^2\frac{\partial S_2}{\partial I'(\mathbf{k})} . \tag{3.22}$$

Insert (3.21) into (3.18) and express everything in terms of the new (primed) variables. Up to order λ^2 we find

$$\begin{aligned}H=&H_0(I')+\lambda(\{S_1,H_0\}+H_1)\\&+\lambda^2\left[\left\{S_2-\tfrac{1}{2}\sum_{\mathbf{k}}\frac{\partial S_1}{\partial I'(\mathbf{k})}\frac{\partial S_1}{\partial\theta'(\mathbf{k})},H_0\right\}\right.\\&\left.+\{S_1,H_1\}+\tfrac{1}{2}\{S_1,\{S_1,H_0\}\}\right] ,\end{aligned} \tag{3.23}$$

where $\{\ \}$ denote Poisson brackets with respect to the primed coordinates θ' and momenta I'. Equation (3.23) and its generalization to higher order in λ can be derived more effectively by means of Lie-algebraic methods,[11] as described in Appendix A. We introduce $H_2(I',\theta')$ for the last two terms of the λ^2 coefficient in (3.23),

$$H_2=\{S_1,H_1\}+\tfrac{1}{2}\{S_1,\{S_1,H_0\}\} , \tag{3.24}$$

and perform a decomposition similar to (3.19). Then (3.23) becomes

$$\begin{aligned}H=&H_0(I')+\lambda\langle H_1(I_1',\theta')\rangle+\lambda^2\langle H_2(I',\theta')\rangle\\&+\lambda\left[\sum_{\mathbf{k}}\frac{\partial H_0(I')}{\partial I'(\mathbf{k})}\frac{\partial S_1}{\partial\theta'(\mathbf{k})}+\tilde{H}_1(I',\theta')\right]\\&+\lambda^2\left[\sum_{\mathbf{k}}\frac{\partial H_0(I')}{\partial I'(\mathbf{k})}\frac{\partial S_2'}{\partial\theta'(\mathbf{k})}+\tilde{H}_2(I',\theta')\right]+O(\lambda^3) ,\end{aligned} \tag{3.25}$$

with

$$S_2'=S_2-\tfrac{1}{2}\sum_{\mathbf{k}}\frac{\partial S_1}{\partial I'(\mathbf{k})}\frac{\partial S_1}{\partial\theta'(\mathbf{k})} . \tag{3.26}$$

This gives the conditions on S_1 and S_2':

$$\sum_{\mathbf{k}} \omega(\mathbf{k}) \frac{\partial S_1}{\partial \theta'(\mathbf{k})} + \tilde{H}_1(I',\theta') = 0 , \tag{3.27}$$

$$\sum_{\mathbf{k}} \omega(\mathbf{k}) \frac{\partial S_2'}{\partial \theta'(\mathbf{k})} + \tilde{H}_2(I',\theta') = 0 . \tag{3.28}$$

This eliminates the expressions in large parentheses in (3.25). The main feature of the resulting Hamiltonian is that the dependence upon the $\theta'_>$ has been removed up to the order λ^3, i.e., the $I'_>$ are constants (adiabatic invariants) up to this order. It is clear that this procedure could, in principle, be carried through in higher order λ, but we will argue below that, when working in $3-\epsilon$ dimensions, there will be a fixed point in λ of order ϵ. Near or at this fixed point we are justified to restrict ourselves to the two lowest-order terms in λ. In the following we shall drop those terms of the Hamiltonian (3.25) which depend only upon the $I_>$, but not on $I_<$ or $\theta_<$. This defines an effective Hamiltonian $H_<$ which describes the motion of the low-momentum degrees of freedom in the presence of a set of adiabatic invariants for the large-momentum modes:

$$H_< = H_{0<}(I') + \lambda \langle H_1(I',\theta') \rangle' + \lambda^2 \langle H_2(I',\theta') \rangle' . \tag{3.29}$$

The prime symbols $\langle\ \rangle'$ indicate that contributions independent of $I'_<$ and $\theta'_<$ are left out.

Before we continue it may be useful to say a few more words about the averaged terms $\langle H_1 \rangle$ and $\langle H_2 \rangle$. From the definition of H_1 (3.13) one sees that by averaging over all $\theta(\mathbf{k})$ with $\mathbf{k} \in \Lambda_>$ many terms in the sum over momenta are left out. Only those terms where for each $e^{-i\theta(\mathbf{k})}(\mathbf{k} \in \Lambda_>)$ we also find that an $e^{i\theta(-\mathbf{k}')}$ with $\mathbf{k} = -\mathbf{k}'$ (and similarly for the complex conjugate) will contribute to $\langle H_1 \rangle$. In other words, in the four external lines of this four-point vertex either all four-menta belong to $\Lambda_<$ [Fig. 1(a)], or two momenta belong to $\Lambda_<$ and the other two momenta (which then belong to $\Lambda_>$) must be equal and opposite [Fig. 1(b)]; or all momenta belong to $\Lambda_>$, and we must have two pairs of equal and opposite momenta [Fig. 1(c)]. The case where all four-momenta belong to $\Lambda_>$ and all four are equal to one another will be suppressed in the limit $N \to \infty$. In Fig. 1 we illustrate these cases by drawing "Feynman" diagrams: the averaging procedure which we are using in order to eliminate dependence upon the $\theta_>$ leads to expressions which are identical to "loops" in perturbation theory of quantum field theory. For an exact comparison one has to use "old-fashioned" perturbation theory (and not covariant perturbation theory), because we are working with the Hamiltonian and not the Lagrangian formulation. The fact that "loops" appear in our classical treatment may, at first sight, look somewhat surprising. One should, however, bear in mind that the main effect of these "loop" corrections is a modification of oscillation frequencies and the nonlinearity parameter λ, and not the introduction of higher harmonics. The latter one would rather associate with "tree diagrams." A detailed derivation and listing of "Feynman rules" is given in Appendix B.

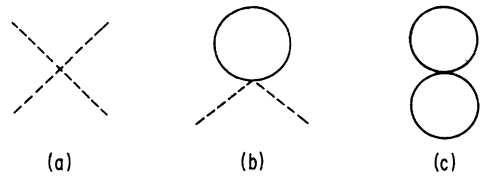

FIG. 1. Contributions associated with $\langle H_1 \rangle$ fall into three classes. (a) All four lines belong to $\Lambda_<$ (slow modes) which are treated as external lines. (b) Two of the lines belong to $\Lambda_<$ and the other two belong to $\Lambda_>$ (fast modes). The contraction of the fast lines gives rise to a loop. (c) All four lines belong to $\Lambda_>$ and their contractions give rise to two loops. In these and the subsequent graphs, dashed lines represent slow modes and solid lines represent fast modes.

The remaining three steps of our renormalization-group transformation will be designed to bring the Hamiltonian (3.29) more precisely into a form which allows comparison with the starting Hamiltonian (3.13). Let us first look at the free part $H_{0<}(I')$ and all those terms in $\langle H_1 \rangle$ where two of the external legs carry momenta of $\Lambda_<$. They are of the form

$$H_{0<} = \sum_{\mathbf{k} \in \Lambda_<} \omega(\mathbf{k}) a'(\mathbf{k}) a'^*(\mathbf{k}) + \tfrac{1}{2} \sum_{\mathbf{k} \in \Lambda_<} \frac{1}{2\omega(\mathbf{k})} [a'(\mathbf{k}) + a'^*(-\mathbf{k})] \times [a'(-\mathbf{k}) + a'^*(\mathbf{k})] \Sigma(\mathbf{k}, I_>) \tag{3.30}$$

[$\Sigma(\mathbf{k}, I_>)$ will be given below]. Here we have used the variables $a'(\mathbf{k}), a'^*(\mathbf{k})$ rather than $I'(\mathbf{k}), \theta'(\mathbf{k})$, because it will simplify our calculations. We perform the Bogoliubov transformation (which is canonical),

$$a''(\mathbf{k}) = \alpha(\mathbf{k}) a'(\mathbf{k}) + \beta(\mathbf{k}) a'^*(-\mathbf{k}) , \quad \alpha^2(\mathbf{k}) - \beta^2(\mathbf{k}) = 1 , \tag{3.31}$$

and (3.30) becomes

$$H_{0<} = \sum_{\mathbf{k} \in \Lambda_<} \omega''(\mathbf{k}) a''(\mathbf{k}) a''^*(\mathbf{k}) , \tag{3.32}$$

with

$$\omega''^2(\mathbf{k}) = \omega^2(\mathbf{k}) + \Sigma(\mathbf{k}, I_>) . \tag{3.33}$$

The transformation (3.31) has the property that

$$\frac{1}{\sqrt{2\omega(\mathbf{k})}} [a'(\mathbf{k}) + a'^*(-\mathbf{k})] = \frac{1}{\sqrt{2\omega''(\mathbf{k})}} [a''(\mathbf{k}) + a''^*(-\mathbf{k})] . \tag{3.34}$$

This implies that the other parts of $\langle H_1 \rangle$ and $\langle H_2 \rangle$ will not change under this transformation (up to corrections of order λ^3). We mention that contributions from $\langle H_2 \rangle$ with two external low momenta are not exactly of the form (3.30), but can also be handled by a Bogoliubov

transformation (see Appendix B). The main result of the transformation (3.31) is a change in the frequencies $\omega(\mathbf{k})$ for $\mathbf{k}\in\Lambda_<$:

$$\omega''(\mathbf{k})^2=m^2+\Sigma(0,I'_>)+4\sum_{i=1}^{3}\sin^2\frac{k_i}{2}+\Sigma(\mathbf{k},I'_>)-\Sigma(\mathbf{0},I'_>)\ . \tag{3.35}$$

The second term defines a change of the mass; that is why this canonical transformation is called "mass renormalization." To make the definition of the renormalized mass precise, we also have to look at the last terms of (3.35). Although in the actual calculation presented below it will turn out that under our approximation $\Sigma(\mathbf{k},I_>)$ does not depend upon $\mathbf{k}$, let us pretend, for the general argument, that $\Sigma(\mathbf{k})-\Sigma(0)\neq 0$. Let us further anticipate that eventually the volume of our lattice will be large (i.e., $N\gg 1$) and the renormalization-group transformation will be repeated many times. Then the momenta $\mathbf{k}\in\Lambda_<$ will eventually be very small and (3.35) will approximately be

$$\omega''(\mathbf{k})^2=m^2+\Sigma(0,I'_>)+\mathbf{k}^2+\mathbf{k}^2\Sigma'(0,I'_>)+O[(k^2)^2]\approx Z^{-1}\{[m^2+\Sigma(0,I'_>)]Z+\mathbf{k}^2\}\ , \tag{3.36}$$

with

$$Z^{-1}=1+\Sigma'(0,I'_>)\ . \tag{3.37}$$

So we define the renormalized mass and frequency:

$$m_R^2=[m^2+\Sigma(0,I'_>)]Z\ , \tag{3.38}$$

$$\omega_R^2(\mathbf{k})=m_R^2+\mathbf{k}^2=Z\omega''^2(\mathbf{k})\ . \tag{3.39}$$

For small momenta $\mathbf{k}$, $\omega_R^2(\mathbf{k})$ is of the same form as our "bare" frequency $\omega^2(\mathbf{k})$ in (3.5). Inserting this into our Hamiltonian (3.29), we obtain the new free part of Hamiltonian (3.23) as

$$(H_<)_0=Z^{-1/2}\sum_{\mathbf{k}\in\Lambda_<}\omega_R(\mathbf{k})I''(\mathbf{k})\ . \tag{3.40}$$

Obviously, another canonical transformation ("wave-function renormalization"),

$$S(I''',\theta''')=Z^{1/2}\sum_{\mathbf{k}\in\Lambda_<}I(\mathbf{k})'''\theta(\mathbf{k})''\ , \tag{3.41}$$

is needed in order to make (3.40) look like the free part of (3.13). Then (3.40) becomes

$$(H_<)_0=\sum_{\mathbf{k}\in\Lambda_<}\omega_R(\mathbf{k})I'''(\mathbf{k})\ , \tag{3.42}$$

which is (almost) of the form we want. Note that under (3.41)

$$\theta''(\mathbf{k})=Z^{-1/2}\theta'''(\mathbf{k})\ , \tag{3.43}$$

we then rescale the time variable

$$t_R=Z^{-1/2}t \tag{3.44}$$

and rename $\theta'''(\mathbf{k})Z^{-1/2}$ as $\theta(\mathbf{k})'''$. The transformation (3.41) also affects those parts of $\langle H_1\rangle'$ and $\langle H_2\rangle'$ which we have not discussed so far: these are contributions where four or six external lines have low momenta $\in\Lambda_<$. It will be shown below that for each such line there is a factor $\sqrt{2I''(\mathbf{k})/\omega''(\mathbf{k})}$ [before the transformation (3.41)]. Using (3.39) and (3.41), each line obtains a factor $Z^{1/2}$. This suggests that one defines renormalized four and six-point interaction terms:

$$V_{4\,\mathrm{ren}}=Z^2V_4\ ,\qquad V_{6\,\mathrm{ren}}=Z^3V_6\ , \tag{3.45}$$

where V_4 and V_6 will be given and discussed below.

These last two canonical transformations, (3.31) and (3.41), are the classical analogs of renormalizations in quantum field theory. As we have made clear, these transformations have been motivated by our demand that the new Hamiltonian (3.29) should be cast into a form where it can be compared to the starting Hamiltonian (3.13). The final step in our renormalization-group transformation consists of a scaling of all dimensional quantities by a factor 2^d, where d is the canonical dimension [we use (length)$=-1$, (momentum)$=1$]. The reason for this lies in the fact that in (3.40) the summation over $\mathbf{k}$ extends over a region different from that in (3.13). We therefore rescale

$$\mathbf{k}=\tfrac{1}{2}\bar{\mathbf{k}} \tag{3.46}$$

and put

$$\omega_R^2(\mathbf{k})=\tfrac{1}{4}\bar{\omega}^2(\bar{\mathbf{k}})\ , \tag{3.47}$$

$$\bar{\omega}^2(\bar{\mathbf{k}})=4m_R^2+16\sum_{i=1}^{3}\sin^2\frac{\bar{k}_i}{4}\ . \tag{3.48}$$

In (3.48) we again anticipate that $\bar{\mathbf{k}}$ will eventually be so small that the second term in (3.48) becomes $\bar{\mathbf{k}}^2$. The free part (3.40) of the Hamiltonian then reads

$$\tfrac{1}{2}{\sum_{\mathbf{k}\in\Lambda}}'\bar{\omega}(\bar{\mathbf{k}})I'''(\tfrac{1}{2}\bar{\mathbf{k}})\ . \tag{3.49}$$

The prime at the summation symbol indicates that in the summation over $\bar{\mathbf{k}}$ the density of points has been thinned out:

$$\bar{\mathbf{k}}=\frac{\pi}{L}\mathbf{n},\ \mathbf{n}=(n_1,n_2,n_3),|n_i|\le N \tag{3.50}$$

with n_i taking only even values. Since the new Hamiltonian describes the physics on a lattice with only half the length of the old one, we simply rewrite (3.50) as

$$\bar{\mathbf{k}}=\frac{2\pi}{L}\bar{\mathbf{n}},\ \ \bar{\mathbf{n}}=(\bar{n}_1,\bar{n}_2,\bar{n}_3),|\bar{n}_i|\le N/2=\frac{\pi}{\bar{L}}\bar{\mathbf{n}},\ \ \bar{L}=\frac{L}{2}\ . \tag{3.51}$$

Similarly, in the interaction part of our Hamiltonian (3.13) we rescale all dimensional quantities by 2^d where d is the canonical dimension. [Note, in particular, that with our definitions (3.6) and (3.10) the action variables $I(\mathbf{k})$ are dimensionless]; the dimension of the coupling constant is

$$[\lambda]=3-D\ , \tag{3.52}$$

which would be $[\lambda]=4-D$ if D were the number of space dimensions $+1$.

This completes our general description of a renormalization-group transformation. The differences between our starting Hamiltonian (3.13) and the new Hamiltonian are the renormalization of frequencies and the coupling constant and the appearance of a higher-order interaction term with six external legs. Before we discuss this in more detail we first have to carry out the actual calculations.

B. One-loop calculations

We begin with $\langle H_1\rangle$, the average over the fast θ's in the interaction part of (3.13). The three contributions are illustrated in Figs. 1(a)–1(c). In order to contribute to $\langle H_1\rangle$, one of the three conditions must be satisfied. (a) All external lines belong to $\Lambda_<$. (b) Two of the lines belong to $\Lambda_>$, say $\mathbf{k}_3$ and $\mathbf{k}_4$. Then we must have $\mathbf{k}_3=-\mathbf{k}_4$. (c) All four momenta belong to $\Lambda_>$. We then need two pairs of equal and opposite momenta, sat, $\mathbf{k}_1=-\mathbf{k}_2$ and $\mathbf{k}_3=-\mathbf{k}_4$. The corresponding expressions are [cf. Eq. (B6)]

$$\langle H_1\rangle_{1(a)}=\frac{1}{L^D 4!}\sum_{\{\mathbf{k}\}\in\Lambda_<}\prod_{j=1}^{4}\frac{1}{\sqrt{2\omega(\mathbf{k}_j)}}[\sqrt{I'(\mathbf{k}_i)}e^{-i\theta'(\mathbf{k}_i)}+\sqrt{I'(-\mathbf{k}_i)}e^{i\theta'(-\mathbf{k}_i)}]\ , \tag{3.53}$$

$$\langle H_1\rangle_{1(b)}=\frac{1}{L^D\times 2}\sum_{\mathbf{k}\in\Lambda_>}\frac{I'(\mathbf{k})}{2\omega(\mathbf{k})}\sum_{\mathbf{k}_1=-\mathbf{k}_2}\prod_{i=1}^{2}\frac{1}{\sqrt{2\omega(\mathbf{k}_i)}}[\sqrt{I'(\mathbf{k}_i)}e^{-i\theta'(\mathbf{k}_i)}+\sqrt{I'(-\mathbf{k}_i)}e^{i\theta'(-\mathbf{k}_i)}]\ , \tag{3.54}$$

and

$$\langle H_1\rangle_{1(c)}=\frac{1}{L^D\times 2}\left[\sum_{\mathbf{k}\in\Lambda_>}\frac{I'(\mathbf{k})}{2\omega(\mathbf{k})}\right]^2\ , \tag{3.55}$$

for Figs. 1(a), 1(b), and 1(c), respectively. Obviously, the last of these contributions does not depend upon any of the variables with $\mathbf{k}\in\Lambda_<$, and hence does not contribute to our new Hamiltonian (3.29). Our expression for $\Sigma(\mathbf{k},I_>)$ [cf. Eq. (3.30)] follows from (3.54):

$$\Sigma=\frac{\lambda}{L^D}\sum_{\mathbf{k}\in\Lambda_>}\frac{I'(\mathbf{k})}{2\omega(\mathbf{k})}\ . \tag{3.56}$$

As it had been said before, Σ does not depend upon the external momenta; such a dependence would only occur at the two-loop level (see Appendix B).

For the calculation of $\langle H_2\rangle$, we need to know $\tilde{H}_1$ and S_1. The oscillatory part $\tilde{H}_1$ can be written as (B13)

$$\tilde{H}_1=\frac{1}{L^D 4!}\sum_{\{\mathbf{k}\}}{}'\sum_{\{\tau\}}\prod_{i=1}^{4}\frac{1}{\sqrt{2\omega(\mathbf{k}_i)}}\sqrt{I'(\tau_i\mathbf{k}_i)}e^{-i\tau_i\theta'(\tau_i\mathbf{k}_i)}\ . \tag{3.57}$$

The symbol $\sum'$ indicates that we should leave out all those momentum configurations which have contributed to $\langle H_1\rangle$. The τ_i take the values $+1$ and -1, and we sum over all possibilities. The function S_1 follows from (3.27) [cf. (B16)]:

$$S_1=i\frac{1}{L^D 4!}\sum_{\{\mathbf{k}\}}{}'\sum_{\{\tau\}}\frac{1}{-\tau_1\omega(\mathbf{k}_1)-\cdots-\tau_4\omega(\mathbf{k}_4)}\times\prod_{i=1}^{4}\frac{1}{\sqrt{2\omega(\mathbf{k}_i)}}\sqrt{I'(\tau_i\mathbf{k}_i)}e^{-i\tau_i\theta'(\tau_i\mathbf{k}_i)} \tag{3.58}$$

We now turn to $\langle H_2\rangle$, where H_2 is defined in (3.24). With (3.27), H_2 is conveniently written as

$$H_2=\tfrac{1}{2}\{S_1,\tilde{H}_1\}+\{S_1,\langle H_1\rangle\}\ . \tag{3.59}$$

Details of the following calculations are described in Appendix B. Here we only give a qualitative description of the calculations and quote some of the results. The second term in (3.59) does not contribute at all to $\langle H_2\rangle$, so we only discuss the first Poisson brackets. Before taking the average over the fast angles, it can be viewed as a six-point vertex (Fig. 2), where the "internal line," which connects the four vertex $\tilde{H}_1$ with the four-point function S_1, represents the contraction due to Poisson brackets. Graphically, we denote this by a cross. The momentum along this line can be fast or slow, and the action and the angle variables of this line cancel out as a result of taking the Poisson bracket. Because of the summation over the τ's in both S_1 and $\tilde{H}_1$, there are two contributions to the internal line. If in Fig. 2 time goes from left to right, and if $e^{-i\theta}$ ($e^{+i\theta}$) denotes an incoming (outgoing) line, then the contribution with $\tau=+$ at the S_1 vertex will be named "positive energy," and the contribution with $\tau=-$, "negative energy." The six external lines in Fig. 2 can be either fast or slow, and, because of summation over the τ's, all possible time orderings have to be drawn (Fig. 3). Finally, one has to remember that certain momentum configurations at the $\tilde{H}_1$ and S_1 vertex have to be left out.

Next when we come to the averaging over the fast angles ($\mathbf{k}\in\Lambda_>$), we find four classes of diagrams (Figs. 4–7):

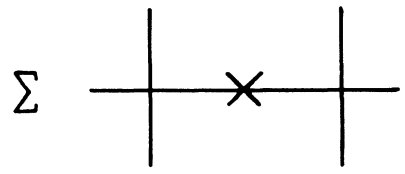

FIG. 2. Graphical representation of H_2 before contraction. The summation is taken over momenta belonging to both the fast and the slow modes.

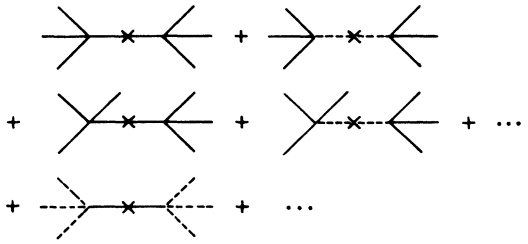

FIG. 3. Decompositions of H_2 according to the fast and the slow momenta, and according to the directions of propagation.

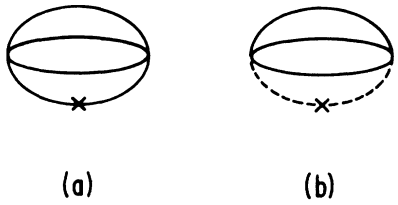

FIG. 4. Graphs with zero external (slow) lines are called vacuum diagrams. These diagrams contribute to the background energy density of the system, and do not affect the dynamics of the slow modes.

graphs with zero, two, four, or six external slow lines. Graphs of the first type ("vacuum diagrams") are not of immediate interest for us: similar to those of Fig. 1(c), they have no dependence upon the $I_<$ and $\theta_<$. The next graph (Fig. 5) provides a two-loop contribution to the two-point function $\Sigma(\mathbf{k},I_>)$. This graph gives the first $\mathbf{k}$-dependent contribution to Σ, but in order to be consistent with our treatment of the four-point function, this two-loop contribution will not be kept. Most important for our goals are the graphs shown in Fig. 6, in particular that of Fig. 6(a). When going from Figs. 2 or 3 to Figs. 4–7 (i.e., when averaging over the fast angles), we again encounter a contraction of two lines ("contraction due to averaging"). The details of this contraction are slightly different from the Poisson-bracket contraction, but there are again two possibilities for such an internal line: it can have either "positive" or "negative" energy (for the definition see above). Graphs with one positive and one negative energy internal lines have no counterpart in quantum field theory. Later on we shall argue that these "wrong" graphs, although they are present in classical canonical perturbation theory, are irrelevant near a fixed point. The same applies to the four-point vertex graph, Fig. 6(b), and the six-point vertex, Fig. 7, which therefore will not be discussed here.

Results for the different time orderings (Fig. 10) of the external lines in Fig. 6(a) are given in Appendix B. Each of them has the form

$$\frac{1}{L^{2D}}\text{const}\lambda^2 \sum_{\{\mathbf{k}\}\in\Lambda_<}{}' \sum_{\{\mathbf{q}\}\in\Lambda_>} \sum_{\substack{\text{external}\\ \text{lines } i=1}}^{4} \frac{1}{\sqrt{2\omega(\mathbf{k}_i)}} \sqrt{I'(\tau_i\mathbf{k}_i)}\, e^{-i\tau_i\theta'(\tau_i\mathbf{k}_i)} \times \frac{1}{2\omega(\mathbf{q}_1)2\omega(\mathbf{q}_2)} \sum_{\{\sigma_1,\sigma_2\}} \frac{\sigma_2 I(\sigma_1\mathbf{q}_1)}{-\sigma_1\omega(\mathbf{q}_1)-\sigma_2\omega(\mathbf{q}_2)-\tau_3\omega(\mathbf{k}_3)-\tau_4\omega(\mathbf{k}_4)} . \tag{3.60}$$

Discrete variables τ (σ) are associated with external (internal) lines, and $\mathbf{k}_i$ ($\mathbf{q}_i$) are external (internal) momenta. In particular, one notices that the sum over all the time orderings cannot be written in the same form as H_2 in (3.53) with λ being replaced by some more complicated one-loop expression because for different time orderings the energies for the external lines come with different signs. In particular, there are "wrong" graphs with $\sigma_1=-\sigma_2$. In order to arrive at the final expression for $V_{4\,\text{ren}}$ in (3.45), we have to take the sum of (a) the graph Fig. 1(a) [Eq. (3.53)] and (b) all orderings of Figs. 6(a) and 6(b) [Eq. (3.60)]. We then have to apply the two canonical transformations associated with the "mass" and the "wave-function" renormalization to the I',θ' variables of the external lines. The former one does not affect the contributions from Figs. 6(a) and 6(b) which have already been of the order λ^2, and because of (3.34) it does not alter the structure of the contribution of Fig. 1(a). The wave-function renormalization pulls out an overall factor $Z^{1/2}$ for each external line which is used to convert V_4 to $V_{4\,\text{ren}}$ in (3.45). The final rescaling of momenta (3.46) and (3.47) for the external momenta, and $1/L^D\to 1/(L/2)^D\times 2^{-D}$ in (3.53) and (3.60) produces an overall factor $\frac{1}{2}\times 2^{3-D}$, where $\frac{1}{2}$ accounts for the overall dimension of H and 2^{3-D} for the dimension of λ.

Our final result for the $H_<$ is then of the form

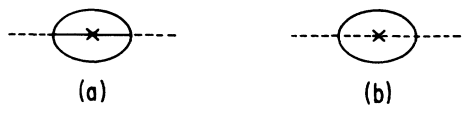

FIG. 5. Graphs with two external (slow) lines are known as self-energy diagrams.

FIG. 6. Graphs with four external lines are known as four-point vertices.

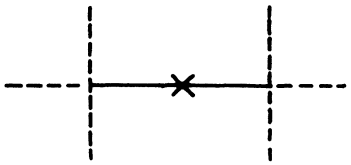

FIG. 7. Graphs with six external lines. The graph with a low-momentum Poisson-bracket contraction is absent in $\langle H_2 \rangle$.

$$H_< = \sum_{\mathbf{k}\in\Lambda}{}' \bar{\omega}(\bar{\mathbf{k}}) I'''(\tfrac{1}{2}\bar{\mathbf{k}}) + V_{4\,\mathrm{ren}} + V_{6\,\mathrm{ren}} , \tag{3.61}$$

where $V_{4\,\mathrm{ren}}$ and $V_{6\,\mathrm{ren}}$ are defined to include the summation over the external momenta $\mathbf{k}_i$. We further remark that all the terms in (3.61) depend upon the $I'_>$, the adiabatic invariants of the fast modes.

IV. FIXED-POINT CONDITIONS

We now turn to the comparison of our starting Hamiltonian (3.13) with the new Hamiltonian (3.61). Under what conditions are they identical (up to the fact that in the first case the lattice length is L, and in the second one, $L/2$)? In answering this question we will follow the arguments outlined in the review paper of Kogut and Wilson.

Let us begin with the free part of the Hamiltonian and compare the frequencies $\omega(\mathbf{k})$ and $\bar{\omega}(\bar{\mathbf{k}})$ [(3.5), (3.39), and (3.48)]. Through our construction of the renormalization-group transformation we have already accomplished that they both have the functional form $\omega^2 = \mathrm{mass}^2 + \mathbf{k}^2$ (for small $\mathbf{k}^2$). Equality of the masses requires that

$$m^2 = 4Z[m^2 + \Sigma(0, I'_>)] . \tag{4.1}$$

Note that Σ is of order λ and also depends upon m^2. This is the analog of Eq. (4.26) in Ref. 1.

Next we turn to the four-point vertex in (3.13) and in (3.61). The contribution corresponding to Figs. 6(a) and 6(b) depends upon the external momenta $\mathbf{k}_1, \ldots, \mathbf{k}_4$ (through the energy denominators), and this dependence differs from one time ordering to another. Since eventually we will be interested only in the region of small external momenta, we approximate this momentum dependence by a Taylor expansion around the renormalization point $\mathbf{k}_1^2 = \cdots = \mathbf{k}_4^2 = 0$. As to the leading term of this expansion where the value of our graphs is evaluated at $\mathbf{k}_1^2 = \cdots = \mathbf{k}_4^2 = 0$, we immediately notice that all contributions to the graph, Fig. 6(b), vanish because of momentum conservation. Their expansions therefore start with terms proportional to $\mathbf{k}_i^2$ or $\mathbf{k}_i \cdot \mathbf{k}_j$. Following Wilson's ϵ expansion and his arguments on irrelevent operators, we shall argue below that such terms are not important near a fixed point. We therefore will not discuss them any further. The same also holds for the six-point graph of Fig. 7.

Before we can state our final results for the diagram, Fig. 6(a), we have to discuss those contributions where one of the internal lines has "negative energy." We shall argue that they also turn out to be unimportant at the fixed point, although for different reasons. We have to remember that in both S_1 and $\tilde{H}_1$ we were instructed to leave out all those momentum configurations where $\mathbf{q}_1 = -\mathbf{q}_2$ (they are part of $\langle H_1 \rangle$): this only applies if $\mathbf{k}_3 + \mathbf{k}_4 = \mathbf{q} = 0$, and it guarantees that there are no divergent terms in the sum over momenta. Now let us anticipate that the lattice is taken so large that sums over momenta are approximated by integrals. A typical example is ($-\mathbf{k}_1 - \mathbf{k}_2 = \mathbf{q} = \mathbf{k}_3 + \mathbf{k}_4$):

$$\int_{\mathbf{q}_1\in\Lambda_>} d^3q_1 \frac{1}{(2\pi)^3} \frac{1}{2\omega(\mathbf{q}_1)2\omega(\mathbf{q}-\mathbf{q}_1)} \frac{[\omega(\mathbf{q}-\mathbf{q}_1)-\omega(\mathbf{q}_1)][I'(\mathbf{q}-\mathbf{q}_1)-I'(\mathbf{q}_1)]}{[\omega(\mathbf{q}-\mathbf{q}_1)-\omega(\mathbf{q}_1)]^2-[\omega(\mathbf{k}_3)-\omega(\mathbf{k}_3-\mathbf{q})]^2} . \tag{4.2}$$

At $\mathbf{q}=0$ we are instructed to subtract from (4.2) the same expression, so the value is zero. On the other hand, if we make the assumption that $I(\mathbf{k})$ is a reasonably well-behaved function of $\mathbf{k}$, both the numerator and the denominator in (4.2) vanish at the same rate as $\mathbf{q}\to 0$, and the integral is finite and generally nonzero at $\mathbf{q}=0$. Therefore, the subtraction is not relevant in the large-volume limit, as a result of $I(\mathbf{k})$ being a smooth function. This seems to imply that those "wrong" contributions to Fig. 6(a) (which have no counterpart in the quantum field theory) give a finite contribution at the point $\mathbf{k}_1^2 = \cdots = \mathbf{k}_4^2 = 0$. Note, however, that when $\mathbf{q}\to 0$ in (4.2) the numerator is proportional to $\partial I(\mathbf{q}_1)/\partial \mathbf{q}_1^2$. For a general trajectory this derivative will be of the same order as I itself, but below we shall find that near a fixed point only those trajectories with small $\partial I/\partial \mathbf{q}_1$ [of order $O(\epsilon^2)$] will survive. This makes (4.2) much smaller than the other contributions to Fig. 6(a) and we will not consider them any more.

At the point $\mathbf{k}_1^2 = \cdots = \mathbf{k}_4^2 = 0$ we are then left with only those contributions to Fig. 6(a) where the internal lines have either both positive or both negative energies. From the energy denominators of the external lines we either have $2m^2$ or zero, so different time orderings still give different results. This difference will disappear if either m^2 is zero or small compared to the rest of the energy denominator, $\omega(\mathbf{q}_1)+\omega(\mathbf{q}_2) \sim \mathbf{q}_1^2 + \mathbf{q}_2^2$. We shall argue below that, in order to get our fixed point of interest, we have to work in $D = 3-\epsilon$ dimensions and to use the ϵ expansion. Then the fixed-point value for m^2 will be of the order ϵ and, hence, small against $\omega(\mathbf{q}_1)+\omega(\mathbf{q}_2)$. Under this condition it is then self-consistent to drop m^2 everywhere in all our graphs contributing to Fig. 6(a). Now they all are of the same form and can be summed up to

$$-\tfrac{1}{4}\prod_{j=1}^{4}\frac{1}{\sqrt{2\omega(\mathbf{k}_j)}}[\sqrt{I(\mathbf{k}_j)}e^{-i\theta(\mathbf{k}_j)}+\sqrt{I(-\mathbf{k}_j)}e^{i\theta(-\mathbf{k}_j)}]\lambda^2$$
$$\times\int_{\mathbf{q}_1\in\Lambda_>}\frac{d^3q_1}{(2\pi)^3}\frac{1}{2\omega(\mathbf{q}_1)}\frac{1}{2\omega(\mathbf{q}-\mathbf{q}_1)}\frac{I'(\mathbf{q}_1)}{\omega(\mathbf{q}_1)+\omega(\mathbf{q}-\mathbf{q}_1)}\ . \tag{4.3}$$

If we denote the integral in the last line by $\mathcal{M}(I_>)$, we have, as a condition for a fixed point

$$\lambda=2^{3-D}Z^2[\lambda-\lambda^2\mathcal{M}(I'_>)]\ . \tag{4.4}$$

This is the analog of Eq. (4.26) in Ref. 1, and again we have indicated that $\mathcal{M}$ depends upon the invariants of the fast modes.

An obvious but trivial solution to Eqs. (4.1) and (4.4) is $m=0$, $\lambda=0$. A more interesting situation arises if we continue all our expressions (where, in the large-volume limit, all discrete sums over momenta are written as momentum integrals) to $D=3-\epsilon$ dimensions and expand in powers of ϵ. To lowest order we find the fixed-point values

$$m^{*2}=-\tfrac{4}{3}\Sigma(0,I'_>)\ ,$$
$$\lambda^*=\epsilon\frac{\ln 2}{\mathcal{M}(I'_>)} \tag{4.5}$$

[note that $\Sigma=O(\lambda)$, hence $m^{*2}=O(\epsilon)$]. The most remarkable difference between our result (4.5) and the analogous result in Ref. 1 is that our fixed-point solution depends upon the invariants of the fast modes which, so far, can be chosen freely.

Let us come back now to all the other contributions to the four-point vertex described in Figs. 6(a) and 6(b) that we have disregarded so far, and also to the six-point function in Fig. 6. As we have already mentioned before, Ref. 1 contains a detailed discussion about why those contributions, to the leading order in ϵ, do not affect the fixed-point values (4.5). The same arguments can also be applied to our situation, and there is no need to repeat them here.

This then completes our answer to the question which we have raised in the beginning of this section. Under the condition that the parameters λ and m^2 are tuned to the values (4.5), we have found that our new Hamiltonian (3.61), describing the dynamics of the $I_<,\theta_<$ variables, is of exactly the same form as our starting Hamiltonian (3.13) which described all the I's and θ's. The fact that m^*,λ^* in (4.5) depend upon the $I'_>$ merely says that the behavior of the $I_<,\theta_<$ cannot be independent of the fast degrees of freedom which form part of the initial conditions.

Let us now turn to the second question: Under what condition can we iterate this renormalization-group transformation without leaving the fixed point? From the fixed-point conditions (4.5) it is quite obvious that such an iteration can only be performed if the action variables I obey a certain restriction. Suppose that λ and m^2 have been tuned to satisfy (4.5) for a certain set of $I_>$'s. Then after the first transformation the Hamiltonian is essentially unchanged. Now repeat the renormalization-group transformation, and again arrive at the conditions (4.1) and (4.4). But now the $I'_>$ which enter into these conditions belong to a set of smaller momenta $\Lambda_>^{(2)}$,

$$\Lambda_>^{(2)}=\Lambda_<^{(1)}-\Lambda_<^{(2)}\ , \tag{4.6}$$

where $\Lambda_>^{(1)}=\Lambda_>$ from (3.16) and

$$\Lambda_>^{(2)}=\left\{\mathbf{k}\,|\,0\le|k_x|,|k_y|,|k_z|\le p^2\frac{\pi}{a}\right\} \tag{4.7}$$

[compare (4.7) with (3.16)]. But now λ and m^2 have been fixed already. They will satisfy the fixed-point conditions (4.1) and (4.4) of the second step only if Σ and $\mathcal{M}$ calculated with the $I'(\mathbf{k}\in\Lambda_>^{(2)})$ are the same as those calculated with the $I'(\mathbf{k}\in\Lambda_>^{(1)})$. So there must be some relation between the invariants I of $\mathbf{k}\in\Lambda_>^{(1)}$ and that of $\mathbf{k}\in\Lambda_>^{(2)}$ or, more generally, a restriction on the field variables $\phi_\mathbf{k}$ as a function of $\mathbf{k}$.

To discuss this in some detail, we introduce

$$\Lambda_>^{(n)}=\left\{\mathbf{k}\,|\,0\le|k_x|,|k_y|,|k_z|\le p^n\frac{\pi}{a}\right\},\quad p=\tfrac{1}{2} \tag{4.8}$$

and

$$\Lambda_>^{(n)}=\Lambda_<^{(n-1)}-\Lambda_<^{(n)}\ . \tag{4.9}$$

With the nth renormalization-group transformation we then average over the angles θ belonging to momenta $\mathbf{k}\in\Lambda_>^{(n)}$ (we have to assume that our lattice is large enough such that after the nth step there are still sufficiently many degrees of freedom left). Let us now follow what happens to our field variables ϕ_k when we iterate the transformation described in Sec. III. Begin with the region $\Lambda_>^{(1)}$ (which is our former $\Lambda_>$). Its field variables $\phi_\mathbf{k}$ are initially given by (3.12). After the first step of the first renormalization-group transformation it changes to

$$\phi_\mathbf{k}=\frac{L^{D/2}}{\sqrt{2\omega(\mathbf{k})}}[\sqrt{I'(\mathbf{k})}e^{-i\theta'(\mathbf{k})}+\sqrt{I'(-\mathbf{k})}e^{i\theta'(-\mathbf{k})}]$$
$$+O(\epsilon)\ . \tag{4.10}$$

The term $O(\lambda)$ contains higher harmonics which mix slow and fast angles, but its overall strength is of order ϵ, and we will not discuss them further. The I' for $\mathbf{k}\in\Lambda_>^{(1)}$ are invariants (up to order ϵ^3). They enter into expressions for $\Sigma(I')$ and $\mathcal{M}(I')$, and they will not be affected by any of the subsequent transformations. For all the other $\mathbf{k}$ (i.e., $\mathbf{k}\in\Lambda_<^{(1)}$ which is our former $\Lambda_<$) the remaining three parts of our first renormalization-group transformation change the ϕ_k from (4.10) into

$$\phi_{\mathbf{k}}=\frac{(L/2)^{D/2}}{\sqrt{2\bar{\omega}(\bar{\mathbf{k}})}}Z^{1/2}2^{D/2}[\sqrt{\bar{I}(\bar{\mathbf{k}})}e^{-i\bar{\theta}(\bar{\mathbf{k}})}+\sqrt{\bar{I}(-\bar{\mathbf{k}})}e^{i\bar{\theta}(-\bar{\mathbf{k}})}]+O(\epsilon) \tag{4.11}$$

(here $\mathbf{k}=\frac{1}{2}\bar{\mathbf{k}}$, and, for the sake of the argument, we include Z, although in our one-loop approximation $Z=1$).

Equation (4.11) is the starting point for the second renormalization-group transformation, and we drop the bars on I, θ, and k. For the region $\mathbf{k}\in\Lambda_{>}^{(2)}$, the averaging part of the second renormalization-group transformation changes (4.11) to

$$\phi_{\mathbf{k}}=\frac{(L/2)^{D/2}}{\sqrt{2\omega(\mathbf{k})}}Z^{1/2}2^{D/2}[\sqrt{I'(\mathbf{k})}e^{-i\theta'(\mathbf{k})}+\sqrt{I'(-\mathbf{k})}e^{i\theta'(-\mathbf{k})}]+O(\epsilon)\ , \tag{4.12}$$

where a new term of order $O(\epsilon)$ which we shall not analyze here has been added. As before, the I' for $\mathbf{k}\in\Lambda_{>}^{(2)}$ are invariants, and they enter into the subsequent calculations of Σ and $\mathcal{M}$. In order to stay on the fixed point, these new Σ and $\mathcal{M}$ must be the same as in the first renormalization-group transformation, so the I' appearing in (4.12) must be related to the I's of (4.10). Since both Σ and $\mathcal{M}$ involve integrations over internal momenta $\mathbf{q}$, we cannot immediately conclude that the I's of Eq. (4.12) and (4.10) are the same. However, after many iterations of the renormalization-group transformation the integration intervals $\Lambda_{>}^{(n)}$ become smaller and smaller, and we come closer and closer to a strict equality of the I's in (4.10) and (4.12). After the second renormalization group has been completed, for $\mathbf{k}\in\Lambda_{<}^{(2)}$ the $\phi_{\mathbf{k}}$ of (4.12) are changed into

$$\phi_{\mathbf{k}}=\frac{(L/4)^{D/2}}{\sqrt{2\bar{\omega}(\bar{\mathbf{k}})}}Z^{1}2^{D}[\sqrt{\bar{I}(\bar{\mathbf{k}})}e^{-i\bar{\theta}(\bar{\mathbf{k}})}+\sqrt{\bar{I}(-\bar{\mathbf{k}})}e^{i\bar{\theta}(-\bar{\mathbf{k}})}]+O(\epsilon)\ , \tag{4.13}$$

where now $\bar{\mathbf{k}}=4\mathbf{k}$.

Now it is easy to generalize this to n iterations. For $\mathbf{k}\in\Lambda_{>}^{(n)}$ we find

$$\frac{1}{(L/2^{n-1})^{D/2}}\phi_{\mathbf{k}}=(Z^{1/2}2^{D/2})^{n-1}\frac{1}{\sqrt{2\omega(\bar{\mathbf{k}})}}\times[\sqrt{I'(\bar{\mathbf{k}})}e^{-i\theta'(\bar{\mathbf{k}})}+\sqrt{I'(-\bar{\mathbf{k}})}e^{i\theta'(-\bar{\mathbf{k}})}]+O(\epsilon)\ , \tag{4.14}$$

where $\mathbf{k}=\bar{\mathbf{k}}/2^{n-1}\bar{\mathbf{k}}$ and the I' are (approximately) independent of n. Here we have taken the volume factor to the other side. $(L/2^{n})^{D}$ is the lattice volume after n steps. Note also that $\omega(\mathbf{k})$ appearing in (4.14) does not change with n. By construction, it is always of the form $\bar{\omega}^2=m^2+\bar{\mathbf{k}}^2$, and m^2 stays the same because of the fixed-point condition. If instead of $\phi_{\mathbf{k}}$ we write $\phi(\bar{\mathbf{k}})$ (with $\bar{\mathbf{k}}=2^{n-1}\mathbf{k}$), then (4.14) takes the simple form

$$\frac{1}{\sqrt{V}}\phi(\bar{\mathbf{k}})=(Z^{1/2}2^{D/2})^{n-1}f(\bar{\mathbf{k}})+O(\epsilon)\ , \tag{4.15}$$

with f being independent of n. From (4.14) we obtain for the small-$\mathbf{k}$ behavior of $\phi_{\mathbf{k}}$:

$$\phi_{\mathbf{k}}=\text{const}|\mathbf{k}|^{-(1/2)D-(1/2)\gamma}\frac{\sqrt{I'(\bar{\mathbf{k}})}e^{-i\theta'(\bar{\mathbf{k}})}+\sqrt{I'(-\bar{\mathbf{k}})}e^{i\theta'(-\bar{\mathbf{k}})}}{\sqrt{2\bar{\omega}(\bar{\mathbf{k}})}}+O(\epsilon)\ , \tag{4.16}$$

with the anomalous dimension

$$\gamma=\frac{\ln Z}{\ln 2}\ . \tag{4.17}$$

[We again remind the reader that $Z=1+O(\lambda^2)$, i.e., $\gamma=O(\epsilon^2)$. Therefore, in our approximation $\gamma=0$.] In (4.16) we have assumed that $\mathbf{k}$ is continuous, and ϕ only depends upon $|\mathbf{k}|$ rather than $\mathbf{k}$. Equation (4.16) contains the answer to the question that we have raised above: in order to remain on the fixed point m^*,λ^* after many iterations, the invariants $I_{>}$ of the fast modes cannot be arbitrary. The restriction is expressed most easily for the amplitudes $\phi_{\mathbf{k}}$, and it selects those classical trajectories for which our renormalization procedure can be carried out. From (4.16) we also derive a scaling low for time averages, i.e.,

$$\langle\phi_{\mathbf{k}}^2\rangle=\text{const}|\mathbf{k}|^{-D-\gamma}\ , \tag{4.18}$$

which is the analog of the scaling law of a Green's function in quantum field theory near a critical point.

To complete this part of our analysis we say a few words about the angular velocities and the action variables. In (4.13), the velocities of the $\bar{\theta}$'s with respect to the original time variable t are

$$\dot{\bar{\theta}}(\bar{\mathbf{k}})=Z^{-1/2}\tfrac{1}{2}\bar{\omega}(\bar{\mathbf{k}})+O(\epsilon)\ . \tag{4.19}$$

After n iterations ($\mathbf{k}=\bar{\mathbf{k}}/2^n$), we have

$$\dot{\theta}(\bar{\mathbf{k}})=(Z^{-1/2}\tfrac{1}{2})^{n}\bar{\omega}(\bar{\mathbf{k}})+O(\epsilon)\ , \tag{4.20}$$

where $\bar{\omega}(\bar{\mathbf{k}})$ is independent of n. From this it follows that the angular velocities of $\phi_{\mathbf{k}}$ in (4.16) with respect to the original time variable t scale in k as

$$\dot{\theta}'(\mathbf{k})\sim|\mathbf{k}|^{1+(1/2)\gamma}\bar{\omega}(\bar{\mathbf{k}})\ . \tag{4.21}$$

For the action variables we find, after n steps,

$$\frac{I(\mathbf{k})}{\omega(\mathbf{k})}=(2Z)^{n}\frac{\bar{I}(\bar{\mathbf{k}})}{\bar{\omega}(\bar{\mathbf{k}})}\ , \tag{4.22}$$

with $\bar{I}/\bar{\omega}$ being independent of n. For small $\mathbf{k}$ [but $|\mathbf{k}|\gg m^*=O(\epsilon)$]

$$I(\mathbf{k}) \sim |\mathbf{k}|^{-\gamma} . \tag{4.23}$$

The important implication of this result is that for those trajectories for which our iterative renormalization procedure is applicable the action variables depend only weakly on $\mathbf{k}$: $\partial I/\partial k^2 = O(\epsilon^2)$. In our discussion after (4.2) we have use of this property for arguing that the "wrong" contributions to Fig. 6(a) are small at a fixed point.

Some of the results presented in this section still depend upon the partitions of the range of momenta: $p = \frac{1}{2}$ in (3.15)–(3.17). For many purposes it is much more convenient to introduce infinitesimal renormalization-group transformations and to obtain Callan-Symanzik–type equations. Let us indicate briefly how this is done for our case and how our results change. We have to take the infinite volume limit and replace the discrete momentum variables by continuum momenta. Denote the upper momentum cutoff by Λ and proceed to transform away all modes within the momentum shell $\Lambda - \delta\Lambda < |\mathbf{k}| < \Lambda$. Intuitively, one expects that every loop integral (e.g., Σ or $\mathcal{M}$) is proportional to $\delta\Lambda$. In an actual computation, however, one encounters infrared divergences which require a careful handling. As an example, consider the one-loop contribution to the four-point vertices, as described in (B26)–(B28) of Appendix B [Figs. 10(a)–10(c)]. To obtain the renormalized coupling constant, we evaluate these diagrams at small but nonvanishing external $\mathbf{k}$'s and then send these $\mathbf{k}$'s to zero. Contributions with $\tau_1 = \tau_2$ cause no problems and can be evaluated straightforwardly. The "wrong" term with $\tau_1 = -\tau_2$, however, can lead to infrared divergences [for example, the denominators of (B27) vanish as $\mathbf{k}_1$ and $\mathbf{k}_2 \to 0$]. By taking suitable combinations of such graphs, one arrives at an expression of the type (4.2) which is finite. As $\delta\Lambda \to 0$, a surface term remains which gets canceled only after a slight shifting of the integration boundary surface. We believe that this kind of cancellation occurs in all cases, but we have no proof for that. The deeper reason for this kind of difficulty is the sharp division between momenta which are integrated over and those which are not. This problem is also present in the renormalization procedure of quantum field theory (see Ref. 1), but in our "wrong" contributions which have no quantum analog it appears to be more acute.

Assuming that these difficulties can be handled successfully, we arrive at a well-behaved correction to the four-point function, $-\lambda^2 M(\Lambda, I_>)\delta\Lambda$, where $M(\Lambda, I_>)$ is the derivative with respect to the lower cutoff $\Lambda - \delta\Lambda$ of our integrals. A similar calculation can be done for the self-energy diagrams. As we have mentioned before, in the one-loop level the self-energy does not depend upon $\mathbf{k}^2$ and, hence, does not lead to a wave-function renormalization. In the two-loop approximation, $\mathbf{k}^2$ dependence comes from Fig. 5. Expanding around $\mathbf{k}^2 = 0$, we have

$$\Sigma(\mathbf{k}^2) = \delta m^2 + (Z^{-1} - 1)\mathbf{k}^2 + O(k^4) , \tag{4.24}$$

$$m_R^2 = Z(m^2 + \delta m^2) . \tag{4.25}$$

The β function follows from

$$\lambda_R = Z^2[\lambda - \lambda^2 M(\Lambda, I)\delta\Lambda] , \tag{4.26}$$

$$\beta = -\Lambda \frac{\partial}{\partial \delta\Lambda} \lambda_R . \tag{4.27}$$

The anomalous dimension [cf. (4.17)] is

$$\gamma = -\Lambda \frac{\partial}{\partial \delta\Lambda} \ln Z \approx -\Lambda \frac{\partial}{\partial \delta\Lambda}(Z - 1) . \tag{4.28}$$

We have worked out the one-loop contributions and found that they have the same functional form as those of the quantum $\lambda\phi^4$ theory, with the replacement of $\hbar \to 2I(\mathbf{k})$.

A few words should be said about the dependence of γ and β upon the action variables. As we have said, β depends upon $I(\Lambda)$, so does the fixed-point value λ^* (zero of the β function). The speed by which $\lambda \neq \lambda^*$ either approaches or leaves the fixed-point value λ^*, therefore, depends upon the value $I(\Lambda)$. In γ, however, the two I factors inside the integral cancel against the I factors from replacing $\lambda \to \lambda^*$, and γ is universal.

V. DISCUSSIONS

The main results of our paper are the fixed-point conditions (4.1) and (4.4) and the scaling law (4.14) for the amplitudes $\phi_{\mathbf{k}}$. We interpret them as follows. For values λ and m^2 sufficiently small (or oder ϵ) there exists a special set of classical trajectories for which the iteration of our renormalization-group transformation allows us to carry out perturbation theory to very high orders. The result of these calculations is the behavior (4.14) for $\phi_{\mathbf{k}}$ in the region of small $\mathbf{k}$. These are regular periodic solutions which differ only slightly from those of the unperturbed Hamiltonian. KAM theory tells us that, when going from the free Hamiltonian to the full Hamiltonian, many of the tori are destroyed, but as long as the perturbation strength is not too large, the majority is preserved (with slight distortions). The solutions which we have been considering belong to the preserved ones, but very likely there are many others to which our method does not apply.

It is crucial to address the question of how rigorous our results can be made. The intention of this paper clearly was to outline the idea of renormalization in a classical lattice field theory rather than to present a rigorous proof. As it is well known, KAM theory[4,5] provides rigorous proofs of the existence of KAM tori for systems with a finite number N of degrees of freedom and small perturbation of strength λ. Upper bounds λ_c on λ can be given, such that for $\lambda < \lambda_c$ the existence of KAM tori can be proven. These critical couplings λ_c, however, go to zero when $N \to \infty$.[12] On the other hand, general experience based upon computer calculations seems to indicate that, for finite N, the estimates for λ_c are rather pessimistic; i.e., at values λ for which proofs of existence cannot be given, KAM tori are still preserved. So it may be that (under favorable circumstances) KAM tori exist even in the limit $N \to \infty$. We do not know whether attempts in this direction have been made at all.

Actually we think that it may very well be that in the infinite-volume limit the situation is even better than for

a system with a finite number of degrees of freedom. In classical field theory, the problem of small denominators turns into the problem of (mainly infrared) divergences of momentum integrals. In contrast to quantum field theory, such divergences may arise even in a massive theory. Dangerous diagrams are those where we have combinations of internal lines with both positive and negative energies (examples are given in the preceding sections). We named these diagrams the "wrong" graphs, since they have no counterparts in quantum field theory. However, our analysis has shown (at least for $\langle H_1 \rangle$ and $\langle H_2 \rangle$) that canonical perturbation theory provides a natural principal-value prescription. Furthermore, when suitable combinations of different time orderings are taken, and reasonable assumptions about the smoothness of the functions $I(\mathbf{k})$ are made, then all divergences are successfully avoided. We have checked this only for the first nontrivial order of perturbation theory, but we see a good chance that this will persist to higher orders.

In any case, our analysis can be refined in the following sense. Throughout our paper we have completely ignored the fact that our free Hamiltonian is intrinsically degenerate, i.e., its frequencies do not depend upon the action variables and $\partial^2 H_0/\partial I_1 \partial I_2 = 0$. This has prevented us from being able to follow the line of arguments usually used in KAM theory: one divides the set of all frequencies into "good" ones (sufficiently incommensurable) and "bad" ones (commensurable or weakly incommensurable); then pick a "good" one and adjust, order by order in λ, the action variables accordingly. We believe, however, that this difficulty of our model can be overcome by reordering the perturbation expansion. Namely, we could absorb all vacuum diagrams [e.g., Figs. 1(c) and 4] into the unperturbed Hamiltonian. Then the frequencies acquire a dependence upon the action variables which is of order λ and may be sufficient to avoid the problem of small denominators. We feel strongly that a repeat of our analysis which takes into account these modifications would be very desirable.

Let us next discuss a few implications of our results. A main point is certainly the correspondence between our classical lattice model and its quantum analog (or statistical-mechanics analog). First, it may be worthwhile to again emphasize the close resemblance between the classical canonical perturbation expansion and the perturbation theory in quantum field theory. In both cases, terms in the expansion can be pictured as diagrams with closed momentum loops (Feynman diagrams). Since we are using the Hamiltonian formulation, the exact comparison has to be made with the old-fashioned perturbation theory rather than with the covariant perturbation theory. Furthermore, the expressions for the classical mechanics graphs contain action variables $I(\mathbf{k})$ at exactly those places where in quantum field theory $\hbar$ would appear (which, however, is usually set $=1$ and thus not seen). Secondly, moving somewhat deeper into the dynamics, our analysis shows that certain solutions of the classical system respond to a change of the momentum cutoff in very much the same way as in the quantum system. In particular, the change of the coupling constant λ is governed by a β function which is (up to the appearance of action variables) identical to that of the quantum field theory. The main conceptual difference between the two approaches is that in the classical system we are dealing with individual trajectories. For example, the $I(\mathbf{k})$ dependence of the β function implies that the extent to which λ changes as a function of the momentum cutoff also depends upon the trajectory. The statistical-mechanical system, on the other hand, deals with ensemble averages (expectation values) and, hence, contains less information. The fact that the classical system "knows" about the fixed points, and that on (or near) such a fixed point a distinguished set of classical solutions exhibits a scaling behavior reminiscent of the critical behavior of the quantum system near a critical point hints at a deeper connection between the quantum field theory and the classical field theory than thought previously. Here again our analysis raises questions which should be studied in more detail.

A possible application is the use of the semiclassical approximation for studying the dynamics of quantum field theories such as the confinement problem of Yang-Mills theories. It has been suggested[13] that we use this approximation method for investigating the weak-coupling limit of lattice gauge theories. For small values of the lattice coupling g quantities of physical interest (e.g., the string tension of the mass gap) follow the scaling behavior predicted by the renormalization-group equation and the property of asymptotic freedom. Our findings (when properly generalized and applied to classical lattice gauge theories) seem to imply that, once the renormalization-group equation is already at work at the classical level, there is a good chance to obtain these scaling laws from the semiclassical approximation.

ACKNOWLEDGMENTS

We both wish to express our gratitude to all our colleagues at the Institute for Nonlinear Sciences (INLS) at the University of California, San Diego, La Jolla, where this work has been carried out. Our thanks go, in particular, to the Director of the INLS, Henry D. I. Abarbanel, who has made our visit possible. One of us (J.B.) also wishes to thank Tai Tsun Wu for the long and inspiring discussions which he had with him during a visit to Harvard University. He also acknowledges the financial support of the Deutsche Forschungsgemeinschaft. One of us (S.J.C.) also wishes to thank Jon Wright and members of the La Jolla Institute for their hospitality extended to him during his visit. His research is supported in part by the U.S. National Science Foundation, Grant No. PHY-8701775 and by the La Jolla Institute internal funds.

APPENDIX A: LIE ALGEBRAIC METHOD

For the development of perturbation expansion, it is more convenient to introduce the Lie algebraic method. The derivations are nearly identical to those which appear in quantum perturbation theory. Consider

$$H(q,p) = H_0(q,p) + \lambda H_1(q,p) \,. \tag{A1}$$

We wish to construct a canonical transformation to re-

move the fast angle variables. Using the Lie algebraic method, we can introduce a canonical transformation by

$$q=(\exp C)(q')\equiv q'+\{C,q'\}+\frac{1}{2!}\{C,\{C,q'\}\}+\cdots , \tag{A2}$$

$$p=(\exp C)(p')\equiv p'+\{C,p'\}+\frac{1}{2!}\{C,\{C,p'\}\}+\cdots , \tag{A3}$$

where $\{,\}$ stand for Poisson brackets,

$$\{A,B\}=\sum_i\left(\frac{\partial A}{\partial q_i}\frac{\partial B}{\partial p_i}-\frac{\partial A}{\partial p_i}\frac{\partial B}{\partial q_i}\right) \tag{A4}$$

and $C=C(q',p')$ is a function to be determined. Under the canonical transformation (A2) and (A3), the Hamiltonian in the new coordinates becomes

$$\begin{aligned}H'&=(\exp C)(H(q',p'))\\&=H(q',p')+\{C,H(q',p')\}+\frac{1}{2!}\{C,\{C,H(q',p')\}\}\\&\quad+\cdots .\end{aligned} \tag{A5}$$

A nice property of the Lie algebraic method is that we arrive automatically at an expression of H in terms of the new variables. Since there are no dangers of mixing the new and the old variables, we shall omit the q',p' dependence in (A5) and keep in mind that H and C depend only on the new variables in (A5).

For small λ, we choose C as

$$C=\lambda C_1+\lambda^2C_2+\lambda^3C_3+\cdots . \tag{A6}$$

The new Hamiltonian becomes

$$\begin{aligned}H'&=H_0+\{C,H_0\}+\frac{1}{2!}\{C,\{C,H_0\}\}+\cdots+\lambda H_1\\&\quad+\lambda\{C,H_1\}+\cdots ,\\&=H_0+\lambda(\{C_1,H_0\}+H_1)+\lambda^2(\{C_2,H_0\}+H_2)\\&\quad+\lambda^3(\{C_3,H_0\}+H_3)+\cdots ,\end{aligned} \tag{A7}$$

where

$$H_2\equiv\{C_1,H_1\}+\tfrac{1}{2}\{C_1,\{C_1,H_0\}\} , \tag{A8}$$

$$\begin{aligned}H_3\equiv&\tfrac{1}{2}\{C_2,\{C_1,H_0\}\}+\tfrac{1}{2}\{C_1\{C_2,H_0\}\}\\&+\tfrac{1}{6}\{C_1,\{C_1,\{C_1,H_0\}\}\}\\&+\{C_2,H_1\}+\tfrac{1}{2}\{C_1,\{C_1,H_1\}\} .\end{aligned} \tag{A9}$$

To remove the fast angle variables in H', we separate H_i, $i=1,2,3,\ldots$, into

$$H_i=\langle H_i\rangle+\tilde{H}_i , \tag{A10}$$

where $\langle\ \rangle$ stands for averaging over the fast angle variables, and $\tilde{H}_i$ has zero average value. We shall choose

$$[C_i,H_0]+\tilde{H}_i=0 \tag{A11}$$

giving

$$H'=H_0(q',p')+\lambda\langle H_1\rangle+\lambda^2\langle H_2\rangle+\cdots . \tag{A12}$$

The new Hamiltonian H' depends only on the slow variables and on the action variables associated with the fast variables. Note that variables C_i are related to S_i in Sec. III by

$$C_1=S_1 ,$$

$$C_2=S_2-\frac{1}{2}\frac{\partial S_1}{\partial I_i}\frac{\partial S_1}{\partial\theta_i} .$$

APPENDIX B: SECOND-ORDER PERTURBATION CALCULATIONS IN THE $\lambda\phi^4$ FIELD THEORY AND THE DIAGRAMMATICAL RULES

1. Diagrammatical rules

In this appendix, we work out the second-order perturbation calculations in the $\lambda\phi^4$ field thoery. The Hamiltonian for a discretized version of the $\lambda\phi^4$ field theory is given in Sec. III as

$$H=H_0+\lambda H_1 \tag{B1}$$

with

$$H_0=\sum_{\mathbf{k}}\omega(\mathbf{k})a^*(\mathbf{k})a(\mathbf{k}) , \tag{B2}$$

$$H_1=\frac{1}{L^D4!}\sum_{\{\mathbf{k}\}}\prod_{i=1}^{4}\frac{1}{\sqrt{2\omega(\mathbf{k}_i)}}[a(\mathbf{k}_i)+a^*(-\mathbf{k}_i)] , \tag{B3}$$

where a $\delta^3(\sum\mathbf{k})$ is included in the definition of $\sum_{\{\mathbf{k}\}}$. Complex variables a and a^* are the classical analog of the quantum annihilation and creation operators.

To first order, the removal of the fast angle dependences leads to $\lambda\langle H_1\rangle$, where $\langle\ \rangle$ denotes the average over the fast modes. In computing the average, we only need to consider terms with an equal number of fast modes a and a^*. The averaging process follows Wick's expansion

$$\langle a(\mathbf{k}_1)a^*(\mathbf{k}_2)\rangle=\delta_I^3(\mathbf{k}_1-\mathbf{k}_2)I(\mathbf{k}_1) ,$$

$$\begin{aligned}&\langle a(\mathbf{k}_1)a(\mathbf{k}_2)a^*(\mathbf{k}_3)a^*(\mathbf{k}_4)\rangle\\&\quad=\langle a(\mathbf{k}_1)a^*(\mathbf{k}_3)\rangle\langle a(\mathbf{k}_2)a^*(\mathbf{k}_4)\rangle\\&\qquad+\langle a(\mathbf{k}_1)a^*(\mathbf{k}_4)\rangle\langle a(\mathbf{k}_2)a^*(\mathbf{k}_3)\rangle .\end{aligned} \tag{B4, B5}$$

In (B5), we have ignored a term due to $\mathbf{k}_1=\mathbf{k}_2=\mathbf{k}_3=\mathbf{k}_4$. This term is negligible in the infinite-volume limit.

The average of λH_1 has already been computed in Sec. III. It can be summarized as

$$\lambda\langle H_1\rangle=\lambda H_1(\text{all } \mathbf{k}\text{'s } \in\Lambda_<)+\frac{\lambda}{2L^D}\sum_{\mathbf{k}\in\Lambda_>}\frac{I(\mathbf{k})}{2\omega(\mathbf{k})}\sum_{\mathbf{k}_1\in\Lambda_<}\frac{1}{2\omega(\mathbf{k}_1)}[a(\mathbf{k}_1)+a^*(-\mathbf{k}_1)][a(-\mathbf{k}_1)+a^*(\mathbf{k}_1)]$$
$$+\frac{\lambda}{2L^D}\sum_{\mathbf{k}_1\in\Lambda_>}\frac{I(\mathbf{k}_1)}{2\omega(\mathbf{k}_1)}\sum_{\mathbf{k}_2\in\Lambda_>}\frac{I(\mathbf{k}_2)}{2\omega(\mathbf{k}_2)}\ . \tag{B6}$$

These three terms are represented diagramatically in Figs. 1(a)–1(c). In the infinite-volume limit, we replace the loop summation $L^{-D}\sum_{\mathbf{k}}$ by the loop integral $d^3k[1/(2\pi)^3]$, giving

$$\langle H_1\rangle=H_1(\text{all } \mathbf{k}\text{'s } \in\Lambda_<)+\tfrac{1}{2}\int_{\mathbf{k}\in\Lambda_>}d^3k\frac{1}{(2\pi)^3}\frac{I(\mathbf{k})}{2\omega(\mathbf{k})}\sum_{\mathbf{k}_1\in\Lambda_<}\frac{1}{2\omega(\mathbf{k}_1)}[a(\mathbf{k}_1)+a^*(-\mathbf{k}_1)][a(-\mathbf{k}_1)+a^*(\mathbf{k}_1)]$$
$$+\frac{L^D}{2}\left[\int d^3k\frac{1}{(2\pi)^3}\frac{I(\mathbf{k})}{2\omega(\mathbf{k})}\right]^2\ . \tag{B7}$$

The volume factor drops out in the second term which describes a mass term. The third term is a vacuum diagram and is proportional to volume as expected.

Knowing $\langle H_1\rangle$, we obtain $\tilde{H}_1$ trivially as

$$\tilde{H}_1=H_1-\langle H_1\rangle\ . \tag{B8}$$

From $\tilde{H}_1$, we can compute S_1 and H_2 through

$$\{S_1,H_0\}+\tilde{H}_1=0\ , \tag{B9}$$
$$H_2=\tfrac{1}{2}\{S_1,\tilde{H}_1\}+\{S_1,\langle H_1\rangle\}\ . \tag{B10}$$

We find it more convenient to introduce a new set of variables $b(\mathbf{k},\tau)$,

$$b(\mathbf{k},1)=a(\mathbf{k})\ , \tag{B11}$$

$$b(\mathbf{k},-1)=a^*(-\mathbf{k})\ . \tag{B12}$$

The discrete variable τ takes on values ±1, and describes the sign of the frequency (phase factor) of $b(\mathbf{k},\tau)$. In terms of $\mathbf{k}$ and τ, $\tilde{H}_1$ has a compact form,

$$\tilde{H}_1=\frac{1}{L^D4!}\sum_{\{\mathbf{k}\}}{}'\sum_{\{\tau\}}\prod_{i=1}^{4}\frac{1}{\sqrt{2\omega(\mathbf{k}_i)}}b(\mathbf{k}_i,\tau_i)\ . \tag{B13}$$

The symbol $\sum'$ indicates that we have subtracted from H_1 terms associated with $\langle H_1\rangle$. The Poisson brackets between the products of b's and H_0 are

$$i\{b(\mathbf{k},\tau),H_0\}=\tau\omega(\mathbf{k})b(\mathbf{k},\tau)\ , \tag{B14}$$

$$i\left\{\prod_j b(\mathbf{k}_j,\tau_j),H_0\right\}=\sum_i\tau_i\omega(\mathbf{k}_i)\prod_j b(\mathbf{k}_j,\tau_j)\ . \tag{B15}$$

Using (B9), (B13), and (B15), we obtain an S_1 easily as

$$S_1=\frac{1}{L^D4!}\sum_{\{\mathbf{k}\}}{}'\sum_{\{\tau\}}\frac{i}{-\sum_j\tau_j\omega(\mathbf{k}_j)}\prod_{i=1}^{4}\frac{1}{\sqrt{2\omega(\mathbf{k}_i)}}b(\mathbf{k}_i,\tau_i)\ . \tag{B16}$$

We associate mode $b(\mathbf{k},\tau)$ with a wave vector (momentum) $\mathbf{k}$ and a frequency (energy) $\tau\omega(\mathbf{k})$.

The second term in (B10) vanishes after averaging over fast modes. We only need to evaluate the first term $\frac{1}{2}\{S_1,H_1\}$, obtaining

$$H_2=\tfrac{1}{2}\langle\{S_1,\tilde{H}_1\}\rangle=-\tfrac{1}{2}\langle\{\tilde{H}_1,S_1\}\rangle$$
$$=\frac{1}{2L^{2D}(4!)^2}\sum_{\{\mathbf{k}\}}{}'\sum_{\{\tau\}}\sum_{\{\mathbf{k}'\}}{}'\sum_{\{\tau'\}}\frac{-i}{-\sum_j\tau_j\omega(\mathbf{k}_j)}$$
$$\times\left\langle\left\{\prod_i\frac{1}{\sqrt{2\omega(\mathbf{k}'_i)}}b(\mathbf{k}'_i,\tau'_i),\ \prod_j\frac{1}{\sqrt{2\omega(\mathbf{k}_j)}}b(\mathbf{k}_j,\tau_j)\right\}\right\rangle\ . \tag{B17}$$

As before, the symbol $\sum'$ indicates that we need to subtract terms associated with $\langle H_1\rangle$.

We first look at the Poisson brackets in (B17) before averaging over the fast angle variables,

$$\left\{\prod_i b(\mathbf{k}'_i,\tau'_i),\prod_j b(\mathbf{k}_j,\tau_j)\right\}=\sum_l\sum_m\prod_{i(\neq l)}b(\mathbf{k}'_i,\tau'_i)\prod_{j(\neq m)}b(\mathbf{k}_j,\tau_j)\{b(\mathbf{k}'_l,\tau'_l),b(\mathbf{k}_m,\tau_m)\}\ . \tag{B18}$$

Expansion (B18) leads to 16 identical contributions which cancel the 4^2 term in $1/(4!)^2$. There are two nonvanishing types of Poisson brackets: one arises from $\tau=+1$ through $\{a^*(-\mathbf{k}'),a(\mathbf{k})\}=i\delta^2(\mathbf{k}+\mathbf{k}')$, and another from $\tau=-1$ through $\{a(\mathbf{k}'),a^*(-\mathbf{k})\}=-i\delta^3(\mathbf{k}+\mathbf{k}')$. Together with the $1/\sqrt{2\omega(\mathbf{k})}$ factors, this leads naturally to a $\tau/2\omega(\mathbf{k})$ factor associated with the Poisson brackets.

We introduce the following graphical representations. We assign the direction of time as running from left to right. We associate $\tilde{H}_1$ and S_1 with two different vertices. We denote $a^*(\mathbf{k})$ as an outgoing line, $a(\mathbf{k})$ as an incoming line, and the Poisson brackets by a line with a cross on it. See Table I for these graphical representations. The left-hand side of (B18) is a polynomial in b of degree 6. Each of the b's is represented by an external line. Thus, before the average over the fast modes is taken, H_2 is represented by a double cross as shown in Fig. 2.

Next, we consider the average over the fast modes. We need to evaluate the expectation values of b's in (B18). They can be evaluated by Wick's expansions described in (B4) and (B5). We refer to the individual $\langle a^*a\rangle$ factor in this Wick's expansion as a contraction due to the averaging process, and denote it graphically by a solid line without a cross. There are also two kinds of contributions: $\langle a^*(-\mathbf{k}')a(\mathbf{k})\rangle=I(\mathbf{k})\delta^3(\mathbf{k}+\mathbf{k}')$ for $\tau=+1$ and $\langle a(\mathbf{k}')a^*(-\mathbf{k})\rangle=I(-\mathbf{k})\delta^3(\mathbf{k}+\mathbf{k}')$ for $\tau=-1$. This contribution is similar to that of the Poisson brackets except that the amplitude is $I(\tau\mathbf{k})$. In Fig. 8, we describe the contraction diagrams both as old-fashioned perturbation diagrams and as new perturbation diagrams. In our new perturbation diagram, we have subtracted from the old-fashioned diagram a wave from $t=-\infty$ to ∞. In Fig. 8(b), the absence of a wave between two interactions with momentum $-\mathbf{k}$ and energy $\omega(\mathbf{k})$ is now interpreted as the presence of a wave with momentum $\mathbf{k}$ and energy $-\omega(\mathbf{k})$. Note that the momentum is conserved at each vertex. In Fig. 8, if we interchange the time ordering, the

TABLE I. Diagrammatic rules for computing $\lambda^n\langle H_n\rangle$ in the $\lambda\phi^4$ field theory.

Process	*Graphical Representation*	*Amplitude*
External Mode (slow mode)	$\mathbf{k},\tau=1$ ———	$a(\mathbf{k})/\sqrt{2\omega(k)}$
	$\mathbf{k},\tau=-1$ ———	$a^*(\mathbf{k})/\sqrt{2\omega(k)}$
Contraction due to Poisson brackets	$\mathbf{k},\tau$ ——×——	$\tau/2\omega(k)$
Contraction due to average over fast modes	$\mathbf{k},\tau$ ———	$I(\tau k)/2\omega(k)$
Vertex	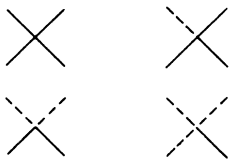	$\lambda\delta_I^3(\Sigma k)/4!$
Energy denominator	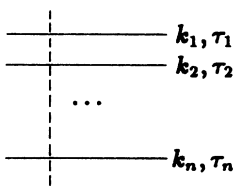	$\dfrac{1}{\sum_{final}\omega(k)-\sum_{int.}\tau\omega(k)}$
n^{th} order prefactor		$(L^{-D})^n/n!$

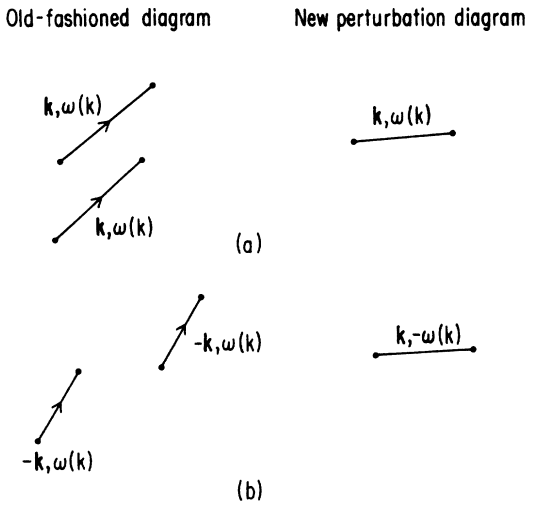

FIG. 8. Graphical representations of contractions in the old-fashioned perturbation diagrams vs those in the new perturbation diagrams. (a) Diagrams with $\tau=1$. (b) Diagrams with $\tau=-1$.

two diagrams will interchange ($\tau\rightarrow-\tau$) if we also change $\mathbf{k}$ to $-\mathbf{k}$. Thus the sum over τ implies a sum over different time orderings.

In $\langle H_2\rangle$, each of the slow modes ($\mathbf{k}\in\Lambda_<$) appears either as an $a(\mathbf{k})$ or an $a^*(\mathbf{k})$. We denote these slow modes graphically by dashed lines and associate them with amplitudes $a(\mathbf{k})/\sqrt{2\omega(\mathbf{k})}$ and $a^*(\mathbf{k})/\sqrt{2\omega(\mathbf{k})}$.

Combining the extra factor i from the Poisson brackets, we have an energy denominator $1/[-\sum_i \tau_i\omega(\mathbf{k}_i)]$ which depends only on the momenta of the S_1 vertex. To express the energy denominator in terms of the final and the intermediate energies, we put the S_1 vertex to the right of the $\tilde{H}_1$ vertex. A summation over τ variables ensures us that we have included contributions for both time orderings. Outgoing particles leaving the S_1 vertex have $\tau=-1$ and are counted in the final states. All incoming and internal particles entering the S_1 vertex are counted as the intermediate states. Other particles not interacting with the S_1 vertex do not contribute to the energy denominator. Then, we can rewrite the energy denominator as

$$\frac{1}{\sum_{\text{final}}\omega(\mathbf{k})-\sum_{\text{inter}}\tau\omega(\mathbf{k})}\ , \tag{B19}$$

which has the same form as in the old-fashioned perturbation theory. The summation over the τ's implies that the intermediate loop energy is not always positive. When all τ's are positive, the energy denominator is the same as the usual old-fashioned perturbation result. When all τ's are negative, it corresponds to the old-fashioned perturbation result with time reversed. The amplitude with a mixture of positive and negative τ's has no simple old-fashioned perturbation interpretation, and it represents a special feature of our theory.

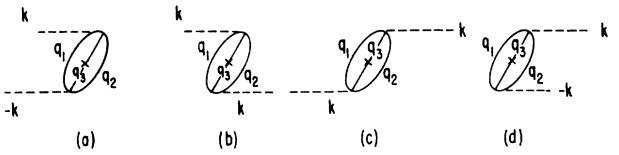

FIG. 9. These four two-loop self-energy diagrams have different time propagation directions of the external legs.

Finally, we need to mention the counting of the equivalent diagrams. The number of possible permutations of the vertices and the contractions cancel part of the factor $1/(4!)^2$. The remaining factor is $1/S$, where S is the degree of symmetry of the diagram, as is the usual perturbation theory.

We summarize these rules in Table I. In computing H', we need to sum over both the internal and the external $\mathbf{k}$ and τ variables. Note that the external legs have a and a^* factors attached. We can read off the n-point amplitudes from the coefficients of the approprate a and a^* monomial terms.

2. Self-energy diagrams

In Fig. 9, we denote the external momentum by $\mathbf{k}(\mathbf{k}\in\Lambda_<)$ and the internal momenta by $\mathbf{q}_1$, $\mathbf{q}_2$, and $\mathbf{q}_3$. The momenta $\mathbf{q}_1$ and $\mathbf{q}_2$ are fast momenta ($\mathbf{q}_1,\mathbf{q}_2\in\Lambda_>$), but $\mathbf{q}_3$ can be either fast or slow. There are four different time-ordered diagrams as shown in Figs. 9(a)–9(d). These bubblelike diagrams have a symmetry factor $\frac{1}{2}$. The amplitudes associated with these diagrams are

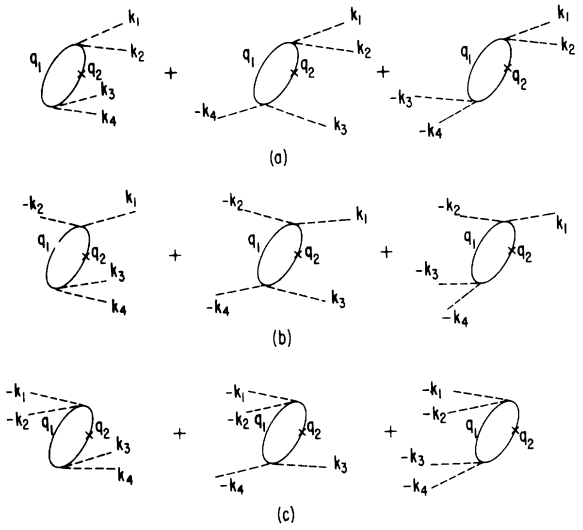

FIG. 10. These nine four-point vertices have different external-leg propagation directions. Diagrams within each category [(a)–(c)] have the same amplitude.

$$\Sigma_{9(a)}=\frac{1}{2}\frac{1}{2L^{2D}}\sum_{\mathbf{k}}\sum_{\{\mathbf{q}\}}'\sum_{\{\tau\}}\delta_I^3\left[\mathbf{k}+\sum\mathbf{q}\right]\frac{1}{2\omega(\mathbf{k})}$$
$$\times\prod_1^3\frac{1}{2\omega(\mathbf{q}_i)}\frac{\tau_3 I(\tau_1\mathbf{q}_1)I(\tau_2\mathbf{q}_2)}{-\omega(\mathbf{k})-\tau_1\omega(\mathbf{q}_1)-\tau_2\omega(\mathbf{q}_2)-\tau_3\omega(\mathbf{q}_3)}a^*(\mathbf{k})a^*(-\mathbf{k})\,, \tag{B20}$$

$$\Sigma_{9(b)}=\frac{1}{2}\frac{1}{2L^{2D}}\sum_{\mathbf{k}}\sum_{\{\mathbf{q}\}}'\sum_{\{\tau\}}\delta_I^3\left[\mathbf{k}+\sum\mathbf{q}\right]\frac{1}{2\omega(\mathbf{k})}$$
$$\times\prod_1^3\frac{1}{2\omega(\mathbf{q}_i)}\frac{\tau_3 I(\tau_1\mathbf{q}_1)I(\tau_2\mathbf{q}_2)}{-\omega(\mathbf{k})-\tau_1\omega(\mathbf{q}_1)-\tau_2\omega(\mathbf{q}_2)-\tau_3\omega(\mathbf{q}_3)}a^*(\mathbf{k})a(\mathbf{k})\,, \tag{B21}$$

$$\Sigma_{9(c)}=\frac{1}{2}\frac{1}{2L^{2D}}\sum_{\mathbf{k}}\sum_{\{\mathbf{q}\}}'\sum_{\{\tau\}}\delta_I^3\left[\mathbf{k}-\sum\mathbf{q}\right]\frac{1}{2\omega(\mathbf{k})}$$
$$\times\prod_1^3\frac{1}{2\omega(\mathbf{q}_i)}\frac{\tau_3 I(\tau_1\mathbf{q}_1)I(\tau_2\mathbf{q}_2)}{\omega(\mathbf{k})-\tau_1\omega(\mathbf{q}_1)-\tau_2\omega(\mathbf{q}_2)-\tau_3\omega(\mathbf{q}_3)}a^*(\mathbf{k})a(\mathbf{k})\,, \tag{B22}$$

$$\Sigma_{9(d)}=\frac{1}{2}\frac{1}{2L^{2D}}\sum_{\mathbf{k}}\sum_{\{\mathbf{q}\}}'\sum_{\{\tau\}}\delta_I^3\left[\mathbf{k}-\sum\mathbf{q}\right]\frac{1}{2\omega(\mathbf{k})}$$
$$\times\prod_1^3\frac{1}{2\omega(\mathbf{q}_i)}\frac{\tau_3 I(\tau_1\mathbf{q}_1)I(\tau_2\mathbf{q}_2)}{\omega(\mathbf{k})-\tau_1\omega(\mathbf{q}_1)-\tau_2\omega(\mathbf{q}_2)-\tau_3\omega(\mathbf{q}_3)}a(\mathbf{k})a(-\mathbf{k})\,. \tag{B23}$$

It is important to note that if we change $\mathbf{q}_i\rightarrow-\mathbf{q}_i$, $\tau_i\rightarrow-\tau_i$, amplitudes $\Sigma_{9(c)}$ and $\Sigma_{9(d)}$ will have the same form as $\Sigma_{9(a)}$ and $\Sigma_{9(b)}$. Thus we have

$$\Sigma=\Sigma_{9(a)}+\Sigma_{9(b)}+\Sigma_{9(c)}+\Sigma_{9(d)}$$
$$=\frac{1}{2}\frac{1}{2L^{2D}}\sum_{\mathbf{k}}\sum_{\{\mathbf{q}\}}'\sum_{\{\tau\}}\delta_I^3\left[\mathbf{k}+\sum\mathbf{q}\right]\frac{1}{2\omega(\mathbf{k})}\prod_1^3\frac{1}{2\omega(\mathbf{q}_i)}\frac{\tau_3 I(\tau_1\mathbf{q}_1)I(\tau_2\mathbf{q}_2)}{-\omega(\mathbf{k})-\tau_1\omega(\mathbf{q}_1)-\tau_2\omega(\mathbf{q}_2)-\tau_3\omega(\mathbf{q}_3)}$$
$$\times[a^*(\mathbf{k})a^*(-\mathbf{k})+2a^*(\mathbf{k})a(\mathbf{k})+a(\mathbf{k})a(-\mathbf{k})]\,. \tag{B24}$$

In addition, if $I(\mathbf{k})=I(-\mathbf{k})$, then the amplitude is the same for $\mathbf{k}$ and $-\mathbf{k}$. Then, we can replace the $2a^*(\mathbf{k})a(\mathbf{k})$ term in (B30) by $a^*(\mathbf{k})a(\mathbf{k})+a^*(-\mathbf{k})a(-\mathbf{k})$, giving

$$\Sigma=\frac{1}{2}\frac{1}{2L^{2D}}\sum_{\mathbf{k}}\sum_{\{\mathbf{q}\}}'\sum_{\{\tau\}}\delta_I^3\left[\mathbf{k}+\sum\mathbf{q}\right]\frac{1}{2\omega(\mathbf{k})}\prod_1^3\frac{1}{2\omega(\mathbf{q}_i)}\frac{\tau_3 I(\tau_1\mathbf{q}_1)I(\tau_2\mathbf{q}_2)}{-\omega(\mathbf{k})-\tau_1\omega(\mathbf{q}_1)-\tau_2\omega(\mathbf{q}_2)-\tau_3\omega(\mathbf{q}_3)}$$
$$\times[a(\mathbf{k})+a^*(-\mathbf{k})][a(-\mathbf{k})+a^*(\mathbf{k})]\,, \tag{B25}$$

which is proportional to $\phi(\mathbf{k})\phi(-\mathbf{k})$ as in the mass term.

3. Four-point vertices

There are nine different time-ordered four-point functions as shown in Fig. 10. We group them into three different sets with the same amplitudes within each set. The external momenta $\mathbf{k}_1$, $\mathbf{k}_2$, $\mathbf{k}_3$, and $\mathbf{k}_4$ are all soft ($\mathbf{k}_i\in\Lambda_<$), and obey the constraint $\sum\mathbf{k}_i=0$. The internal momentum $\mathbf{q}_1$ is fast, and $\mathbf{q}_2$ may be either fast or slow. The momenta are conserved at each vertex. There are no symmetry factors associated with the internal loop. However, there are symmetry factors associated with the extenal legs which will be included in front of the appropriate a and a^* factors.

The amplitudes for these diagrams are

$$\Gamma_{10(a)}=\frac{1}{2L^{2D}}\sum_{\{\mathbf{k}\}}\delta_I^3\left[\sum\mathbf{k}\right]\prod_1^4\frac{1}{\sqrt{2\omega(\mathbf{k}_i)}}$$
$$\times\sum_{\{\mathbf{q}\}}'\sum_{\{\tau\}}\delta_I^3(\mathbf{q}_1+\mathbf{q}_2-\mathbf{k}_1-\mathbf{k}_2)$$
$$\times\prod_1^2\frac{1}{2\omega(\mathbf{q}_i)}\frac{\tau_2 I(\tau_1\mathbf{q}_1)}{\omega(\mathbf{k}_1)+\omega(\mathbf{k}_2)-\tau_1\omega(\mathbf{q}_1)-\tau_2\omega(\mathbf{q}_2)}\frac{1}{2}a(\mathbf{k}_1)a(\mathbf{k}_2)$$
$$\times[\tfrac{1}{2}a(\mathbf{k}_3)a(\mathbf{k}_4)+a(\mathbf{k}_3)a^*(-\mathbf{k}_4)+\tfrac{1}{2}a^*(-\mathbf{k}_3)a^*(-\mathbf{k}_4)]\,, \tag{B26}$$

$$\Gamma_{10(b)}=\frac{1}{2L^{2D}}\sum_{\{\mathbf{k}\}}\delta_I^3\left[\sum\mathbf{k}\right]\prod_1^4\frac{1}{\sqrt{2\omega(\mathbf{k}_i)}}$$
$$\times\sum_{\{\mathbf{q}\}}{}'\sum_{\{\tau\}}\delta_I^3(\mathbf{q}_1+\mathbf{q}_2-\mathbf{k}_1-\mathbf{k}_2)$$
$$\times\prod_1^2\frac{1}{2\omega(\mathbf{q}_i)}\frac{1}{\omega(\mathbf{k}_1)-\omega(\mathbf{k}_2)-\tau_1\omega(\mathbf{q}_1)-\tau_2\omega(\mathbf{q}_2)}a(\mathbf{k}_1)a^*(-\mathbf{k}_2)$$
$$\times[\tfrac{1}{2}a(\mathbf{k}_3)a(\mathbf{k}_4)+a(\mathbf{k}_3)a^*(-\mathbf{k}_4)+\tfrac{1}{2}a^*(-\mathbf{k}_3)a^*(-\mathbf{k}_4)]\ , \tag{B27}$$

$$\Gamma_{10(c)}=\frac{1}{2L^{2D}}\sum_{\{\mathbf{k}\}}\delta_I^3\left[\sum\mathbf{k}\right]\prod_1^4\frac{1}{\sqrt{2\omega(\mathbf{k}_i)}}$$
$$\times\sum_{\{\mathbf{q}\}}{}'\sum_{\{\tau\}}\delta_I^3(\mathbf{q}_1+\mathbf{q}_2-\mathbf{k}_1-\mathbf{k}_2)$$
$$\times\prod_1^2\frac{1}{2\omega(\mathbf{q}_i)}\frac{\tau_2 I(\tau_1\mathbf{q}_1)}{-\omega(\mathbf{k}_1)-\omega(\mathbf{k}_2)-\tau_1\omega(\mathbf{q}_1)-\tau_2\omega(\mathbf{q}_2)}\frac{1}{2}a^*(-\mathbf{k}_3)a^*(-\mathbf{k}_4)$$
$$\times[\tfrac{1}{2}a(\mathbf{k}_3)a(\mathbf{k}_4)+a(\mathbf{k}_3)a^*(-\mathbf{k}_4)+\tfrac{1}{2}a^*(-\mathbf{k}_3)a^*(-\mathbf{k}_4)]\ . \tag{B28}$$

We encounter here three amplitudes different only in the energy denominators and the a and a^* factors.

---

*Permanent address.

[1]J. Kogut and K. Wilson, Phys. Rep. **12C**, 75 (1974).

[2]For a review on the renormalization-group and ϵ-expression methods, see also S. K. Ma, *Modern Theory of Critical Phenomena* (Benjamin, New York, 1976).

[3]For a field theoretical treatment of the renormalization group, see D. J. Amit, *Field Theory, the Renormalization Group and Critical Phenomena* (World Scientific, Singapore, 1984).

[4]This is the famous KAM theorem: A. N. Kolmogorov, Dokl. Akad. Nauk. SSSR **98**, 527 (1954); V. I. Arnold, Russ. Math. Surv. **18**, 85 (1963); J. Moser, Nachr. Akad. Wiss. Goettingen Math. Phys. Kl. **2**, 1 (1962). Among the three, Arnold's paper is most relevant to our application.

[5]V. I. Arnold, *Dynamical Systems III* (Springer-Verlag, New York, 1988).

[6]For a summary of formulas on elliptical functions, see *Handbook of Mathematical Functions,* Natl. Bur. Stand. Appl. Math. Ser. No. 55, edited by M. Abramowitz and I. A. Stegun (U. S. GPO, Washington, D. C., 1965).

[7]J. Kevorkian and J. D. Cole, *Perturbation Methods in Applied Mathematics* (Springer-Verlag, New York, 1981).

[8]The adiabatic approximation described here has been used to study coupled harmonic oscillators obtained from classical Yang-Mills plane-wave solutions. See S. J. Chang, Phys. Rev. D **29**, 259 (1984).

[9]For a review of Poincaré return maps and related topics, see A. J. Lichtenberg and M. A. Lieberman, *Regular and Stochastic Motion* (Springer-Verlag, New York, 1983); V. I. Arnold, *Mathematical Methods of Classical Mechanics* (Springer-Verlag, New York, 1978).

[10]J. D. Bjorken and S. D. Drell, *Relativistic Quantum Fields* (McGraw-Hill, New York, 1965).

[11]For an introduction to the Lie algebraic method, see, e.g., A. J. Dragt and J. M. Finn, J. Math. Phys. **17**, 2215 (1976).

[12]B. V. Chirikov, Phys. Rep. **52**, 263 (1979).

[13]J. Bartels and T. T. Wu, Phys. Rev. D **37**, 2307 (1988); and J. Bartels and T. T. Wu (unpublished).